

University of Wisconsin - Madison

MADPH-95-870

IUHET-294

RAL-95-013

hep-ph/9503204

March 1995

## Quark Singlets: Implications and Constraints

V. Barger<sup>a</sup>, M.S. Berger<sup>b</sup> and R.J.N. Phillips<sup>c</sup>

<sup>a</sup>*Physics Department, University of Wisconsin, Madison, WI 53706, USA*

<sup>b</sup>*Physics Department, Indiana University, Bloomington, IN 47405, USA*

<sup>c</sup>*Rutherford Appleton Laboratory, Chilton, Didcot, Oxon OX11 0QX, UK*

### Abstract

Quarks whose left- and right-handed chiral components are both singlets with respect to the  $SU(2)$  weak-isospin gauge group, offer interesting physics possibilities beyond the Standard Model (SM) already studied in many contexts. We here address some further aspects. We first collect and update the constraints from present data on their masses and mixings with conventional quarks. We discuss possible effects on  $b \rightarrow s\gamma$  and  $Z \rightarrow b\bar{b}$  decays and give fresh illustrations of CP asymmetries in  $B^0$  decays differing dramatically from SM expectations. We analyse singlet effects in grand unification scenarios:  $d$ -type singlets are most economically introduced in  $\mathbf{5} + \mathbf{5}^*$  multiplets of  $SU(5)$ , with up to three generations, preserving gauge coupling unification with perturbative values up to the GUT scale;  $u$ -type singlets can arise in  $\mathbf{10} + \mathbf{10}^*$  multiplets of  $SU(5)$  with at most one light generation. With extra matter multiplets the gauge couplings are bigger; we give the two-loop evolution equations including exotic multiplets and a possible extra

$U(1)$  symmetry. Two-loop effects can become important, threatening unification (modulo threshold effects), perturbativity and asymptotic freedom of  $\alpha_3$ . In the Yukawa sector, top-quark fixed-point behaviour is preserved and singlet-quark couplings have infrared fixed points too, but unification of  $b$  and  $\tau$  couplings is not possible in a three-generation  $E_6$  model.

## I. INTRODUCTION

In addition to the established three generations of quarks in the Standard Model (SM), the possible existence of exotic singlet quarks (whose left and right chiral components are both singlets with respect to the  $SU(2)$  weak isospin gauge group) has been raised in various contexts. It was once questioned whether the  $b$  quark might be such a singlet, with no doublet partner  $t$  [1]. One charge  $-\frac{1}{3}$  singlet quark appears naturally in each 27-plet fermion generation of  $E_6$  Grand Unification Theories (GUTs) [2–4]. Charge  $\frac{2}{3}$  singlet quarks have been variously motivated, as part of a new mass mechanism for top quarks [5] or as part of a new supersymmetric gauge model with natural baryon-number conservation [6]. If they exist, both kinds of singlet quarks can be produced via their strong and electroweak gauge couplings; mixing with standard quarks then allows the mixed mass eigenstates to decay via charged currents (CC) or neutral currents (NC) to lighter quarks  $q$  plus  $W$  or  $Z$  [3,4,7], and also via Yukawa couplings to  $q$  plus Higgs bosons  $H$  [8,9]. Singlet quark production and decay can therefore give characteristic new signals and modifications of old signals, discussed in the literature [3–5,7,8,10–16]. Possible indirect consequences of singlet-quark mixing for flavor-changing neutral currents (FCNC), flavor-diagonal neutral currents (FDNC) and CP violation have also been considered [5,17–26]

In the present paper we address some further aspects of singlet quark physics. We first collect and update the direct and indirect constraints on masses and singlet-doublet mixing from present data, illustrating possible effects on  $b \rightarrow s\gamma$  and  $Z \rightarrow b\bar{b}$  decays and on CP asymmetries in neutral  $B$  decays. We then analyse the impact of  $Q = -\frac{1}{3}$  and  $Q = \frac{2}{3}$  singlet quarks on the renormalization group equations (RGE), on the unification and perturbativity of gauge and Yukawa couplings, and on the exotic matter multiplets in GUT scenarios.

Section II introduces our notation and lists general basic properties of singlet quark couplings and mixings with SM quarks. Section III addresses the  $4 \times 4$  mixing matrix, arising when one singlet mixes with three SM quarks, and extracts the full set of unitarity constraints based on present limits on the CKM submatrix. Section IV discusses the

constraints implied by the absence of identifiable signals from singlet-quark production and decay at present  $e^+e^-$  and  $p\bar{p}$  colliders. Section V considers tree and box diagram contributions to neutral meson-antimeson oscillations and the indirect constraints on singlet-quark mixing from present data. Section VI addresses indirect constraints from FCNC and FDNC decays, including a new more stringent measurement of  $K_L \rightarrow \mu^+\mu^-$  and weak bounds from  $B^0, D^0 \rightarrow \mu^+\mu^-$  limits; the topical cases  $b \rightarrow s\gamma$  and  $Z \rightarrow b\bar{b}$  are discussed here. The global FDNC constraints are comprehensive enough to have useful repercussions via unitarity, for  $d$ -type singlet mixing. Section VII discusses CP asymmetries in neutral  $B$  decays, with new illustrations of how  $d$ -type singlet mixing can give dramatic changes from SM expectations. Section VIII, our major new contribution, analyses the possible roles of singlet quarks in GUT scenarios. We show that  $d$ -type singlets are most economically introduced in  $\mathbf{5} + \mathbf{5}^*$  multiplets of  $SU(5)$ , with up to three generations, preserving gauge coupling unification and perturbativity up to the GUT scale;  $u$ -type singlets can arise in  $\mathbf{10} + \mathbf{10}^*$  multiplets of  $SU(5)$  with at most one light generation. The presence of extra matter multiplets makes the gauge couplings bigger and two-loop effects potentially more important. We give the two-loop evolution equations, including the effects of exotic matter multiplets and a possible additional  $U(1)'$  gauge coupling, and show that two-loop effects can threaten not only unification (where threshold effects may partly compensate) but also perturbativity and asymptotic freedom of  $\alpha_3$  at large scales. In the Yukawa sector, top-quark fixed-point behaviour is preserved and singlet-quark couplings have infrared fixed points too, but unification of  $b$  and  $\tau$  couplings is not possible in a three-generation  $E_6$  model. Finally, Section IX summarizes our conclusions while Appendices A and B contain some technical details.

## II. BASIC PROPERTIES AND NOTATION

We shall generally denote singlet quarks by the symbol  $x$ , and SM quarks by  $q$ . More specifically,  $x_d$  denotes a generic charge  $-\frac{1}{3}$  singlet and  $x_u$  implies charge  $\frac{2}{3}$ . The weak isospin  $T_3$  and hypercharge  $\frac{1}{2}Y$  of the left and right chiral components, characterizing their

SU(2) and U(1) gauge couplings, contrast with SM assignments as follows:

|                | $u_L$         | $d_L$          | $x_{uL}$      | $x_{dL}$       | $u_R, x_{uR}$ | $d_R, x_{dR}$  |
|----------------|---------------|----------------|---------------|----------------|---------------|----------------|
| $T_3$          | $\frac{1}{2}$ | $-\frac{1}{2}$ | 0             | 0              | 0             | 0              |
| $\frac{1}{2}Y$ | $\frac{1}{6}$ | $\frac{1}{6}$  | $\frac{2}{3}$ | $-\frac{1}{3}$ | $\frac{2}{3}$ | $-\frac{1}{3}$ |
| $Q$            | $\frac{2}{3}$ | $-\frac{1}{3}$ | $\frac{2}{3}$ | $-\frac{1}{3}$ | $\frac{2}{3}$ | $-\frac{1}{3}$ |

where  $Q = T_3 + \frac{1}{2}Y$  is the electric charge. The vector and axial couplings to  $Z$  are

|       | $u$   | $d$  | $x_u$                          | $x_d$                         |
|-------|---|--|--------------------------------|-------------------------------|
| $g_V$ | $\frac{1}{4} - \frac{2}{3} \sin^2 \theta_W$ | $-\frac{1}{4} + \frac{1}{3} \sin^2 \theta_W$ | $-\frac{2}{3} \sin^2 \theta_W$ | $\frac{1}{3} \sin^2 \theta_W$ |
| $g_A$ | $-\frac{1}{4}$                              | $\frac{1}{4}$                                |                                |                               |

where  $\theta_W$  is the Weinberg angle. Both SM and singlet quarks are color triplets and have the same couplings to gluons  $g$ . Hence singlet quarks have pure vector gauge couplings to  $g, \gamma, Z$  (and zero coupling to  $W$ ); they are sometimes called “vector-like” or more precisely “vector-singlet” quarks. They do not contribute to chiral anomalies.

(a)  $2 \times 2$  quark mixing example

Yukawa interactions with Higgs fields generate quark masses and mixings. Mixing with conventional quarks provides natural decay channels and is expected at some level, since new quarks are necessarily unstable [27]. Suppose first, for simplicity, that mass eigenstates  $q, x$  arise from the mixing of just one SM quark field  $q'$  with a singlet quark field  $x'$  of the same (unspecified) charge. Then the SM Higgs field  $H$  can generate a  $m' \bar{q}'_L x'_R + \text{h.c.}$  mixing term as well as the usual  $m \bar{q}'_L q'_R + \text{h.c.}$  mass term. A pure singlet mass term  $M \bar{x}'_L x'_R + \text{h.c.}$  requires an isosinglet Higgs field  $S$  with vacuum expectation value  $v_S$  and coupling  $(M/v_S) S \bar{x}'_L x'_R + \text{h.c.}$ ; this field can also generate a  $M' \bar{x}'_L q'_R$  term. We then have the  $2 \times 2$  mass matrix

$$\begin{pmatrix} m & m' \\ M' & M \end{pmatrix} \quad (1)$$

where the rows refer to  $\bar{q}'_L, \bar{x}'_L$  and the columns refer to  $q'_R, x'_R$ . This is diagonalized by independent rotations of  $L$  and  $R$  coordinates, giving quark mass eigenstates  $q$  and  $x$ :

$$q_L = q'_L \cos \theta_L - x'_L \sin \theta_L, \quad q_R = q'_R \cos \theta_R - x'_R \sin \theta_R, \quad (2)$$

$$x_L = q'_L \sin \theta_L + x'_L \cos \theta_L, \quad x_R = q'_R \sin \theta_R + x'_R \cos \theta_R. \quad (3)$$

Since no singlets have yet been discovered, it is natural to assume that the mixing angles  $\theta_L, \theta_R$  are small and  $x$  is much heavier than  $q$  (at least for  $q = u, d, s, c, b$ ), with  $m_q \simeq m$ ,  $m_x \simeq M \gg m, m', M'$ . Then  $q$  and  $x$  are dominated by  $q'$  and  $x'$  components, respectively, with  $\theta_L \simeq m'/M$ ,  $\theta_R \simeq M'/M$ . Note that  $SU(2)_L$  gauge couplings relate exclusively to  $q'_L$  and hence are controlled by the left-handed mixing angle  $\theta_L$  only.

The heavy mostly-singlet quark  $x$  can now decay to  $q''W$  and  $qZ$  via the couplings

$$\mathcal{L}_{xq''W} = -\frac{g}{\sqrt{2}} \sin \theta_L \bar{q}''_L \gamma^\mu W_\mu x_L, \quad (4)$$

$$\mathcal{L}_{xqZ} = -\frac{g_Z}{2} \sin \theta_L \cos \theta_L \bar{q}_L \gamma^\mu Z_\mu x_L. \quad (5)$$

where  $g$  is the  $SU(2)$  gauge coupling,  $g_Z = g/\cos \theta_W$  and  $q''_L$  is the combination of light quarks that couple via  $W$  to  $q'_L$ . Since  $\cos^2 \theta_L \simeq 1$  by assumption, this gives branching fractions in the ratio  $B(x \rightarrow q''W)/B(x \rightarrow qZ) \simeq 2$  up to phase space factors [3]. Furthermore, if the SM Higgs boson is light enough,  $x$  can also decay to  $qH$  via the coupling

$$\mathcal{L}_{xqH} = -\frac{gm'}{2M_W} \bar{q}_L H x_R \simeq -\frac{g \sin \theta_L m_X}{2M_W} \bar{q}_L H x_R. \quad (6)$$

Hence the Higgs decay mode too is scaled by  $\sin \theta_L$ , and the three decay branching fractions are in the ratios [8]

$$B(x \rightarrow q''W) : B(x \rightarrow qZ) : B(x \rightarrow qH) \simeq 2 : 1 : 1 \quad (7)$$

up to phase space factors that are close to 1, if  $m_x \gg M_W, M_Z, M_H, m_q, m_{q''}$ . These ratios can however be altered greatly if this mass ordering does not hold, or if there is large mixing [8,12–14,16].

In general singlet quarks can mix with all SM quarks of the same charge, requiring a more extended formalism. We first consider scenarios with just one new singlet quark.

(b) One  $Q = -\frac{1}{3}$  singlet quark mixing

For the case of one charge  $-\frac{1}{3}$  singlet field, mixing with the three SM fields of this charge, we denote the mass eigenstate by  $d, s, b, x$  where the first three are identified with the known quarks (now carrying hitherto unsuspected singlet components) and  $x$  is still undiscovered. We denote by  $d'_L, s'_L, b'_L$  the three orthonormal linear combinations of left chiral components that are  $SU(2)_L$  doublet partners of the known  $Q = \frac{2}{3}$  fields  $u_L, c_L, t_L$ ; the remaining orthonormal combination  $x'_L$  is an  $SU(2)_L$  singlet, and we can write

$$\begin{pmatrix} d'_L \\ s'_L \\ b'_L \\ x'_L \end{pmatrix} = \begin{pmatrix} V_{ud} & V_{us} & V_{ub} & V_{ux} \\ V_{cd} & V_{cs} & V_{cb} & V_{cx} \\ V_{td} & V_{ts} & V_{tb} & V_{tx} \\ V_{od} & V_{os} & V_{ob} & V_{ox} \end{pmatrix} \begin{pmatrix} d_L \\ s_L \\ b_L \\ x_L \end{pmatrix}. \quad (8)$$

Here the  $4 \times 4$  unitary matrix  $V$  generalizes the Cabibbo-Kobayashi-Maskawa (CKM) matrix  $V_{\text{CKM}}$ . The top three rows of  $V$  control the  $SU(2)_L$  gauge couplings of  $W$  and  $Z$  bosons; the first 3 rows and columns of  $V$  are precisely  $V_{\text{CKM}}$ . The submatrix  $V_{\text{CKM}}$  is generally non-unitary.

The  $Z$  couplings to the  $SU(2)_L$  left-handed doublet and singlet weak eigenstates  $q'_L = d'_L, s'_L, b'_L, x'_L$  are given by

$$\mathcal{L} = -g_Z \sum_{q'} \bar{q}'_L \left( T_3 + \frac{1}{3} \sin^2 \theta_W \right) \gamma^\mu Z_\mu q'_L. \quad (9)$$

Hence the FCNC couplings between the mass eigenstates  $q_i = d, s, b, x$  are

$$\mathcal{L}_{\text{FCNC}} = \frac{1}{2} g_Z \sum_{i \neq j} z_{ij} \bar{q}_i \gamma^\mu Z_\mu q_j, \quad (10)$$

$$z_{ij} = V_{ui}^* V_{uj} + V_{ci}^* V_{cj} + V_{ti}^* V_{tj} = \delta_{ij} - V_{oi}^* V_{oj}, \quad (11)$$

using the unitarity of  $V$ . Thus the FCNC coefficients  $z_{ij}$  are measures of non-unitarity in  $V_{\text{CKM}}$ . The corresponding FDNC couplings are

$$\mathcal{L}_{\text{FDNC}} = g_Z \sum_{i=d,s,b,x} \bar{q}_i \gamma^\mu Z_\mu \left[ \frac{1}{4} z_{ii} (1 - \gamma_5) - \frac{1}{3} \sin^2 \theta_W \right] q_i. \quad (12)$$

Thus for the standard  $d, s, b$  quarks, mixing with  $x$  reduces direct left-handed FDNC by a factor  $(z_{ii} - \frac{2}{3} \sin^2 \theta_W) / (1 - \frac{2}{3} \sin^2 \theta_W)$  and leaves right-handed FDNC unchanged.

Hence for  $m_x > M_W, M_Z$ , the tree-level widths for CC and FCNC decays to light quarks are

$$\Gamma(x \rightarrow q_i W) = \frac{G_F m_x^3}{8\pi\sqrt{2}} \left(1 - \frac{M_W^2}{m_x^2}\right)^2 \left(1 + \frac{2M_W^2}{m_x^2}\right) |V_{ix}|^2, \quad (13)$$

$$\Gamma(x \rightarrow q_j Z) = \frac{G_F m_x^3}{16\pi\sqrt{2}} \left(1 - \frac{M_Z^2}{m_x^2}\right)^2 \left(1 + \frac{2M_Z^2}{m_x^2}\right) |z_{jx}|^2. \quad (14)$$

If  $x$  is heavy enough that all the  $x \rightarrow q_i W$  and  $x \rightarrow q_j Z$  channels are open and all the phase space factors are  $\simeq 1$ , then we can use unitarity to sum over  $i = u, c, t$  and  $j = d, s, b$  and obtain the total CC and FCNC decay widths,

$$\Gamma(CC) \simeq \frac{G_F m_x^3}{8\pi\sqrt{2}} \sum_i |V_{ix}|^2 \simeq \frac{G_F m_x^3}{8\pi\sqrt{2}} (1 - |V_{ox}|^2), \quad (15)$$

$$\Gamma(FCNC) \simeq \frac{G_F m_x^3}{16\pi\sqrt{2}} \sum_j |V_{oj}^*|^2 |V_{ox}|^2 \simeq \frac{G_F m_x^3}{16\pi\sqrt{2}} (1 - |V_{ox}|^2) |V_{ox}|^2. \quad (16)$$

Hence for small mixing ( $|V_{ox}| \simeq 1$ ) we obtain

$$\Gamma(CC)/\Gamma(FCNC) \simeq 2, \quad (17)$$

a result proved earlier for two-quark mixing, modulo phase space factors.

### (c) One $Q = \frac{2}{3}$ singlet quark mixing

Consider now one  $Q = \frac{2}{3}$  singlet field mixing with the SM fields of the same charge and denote the mass eigenstates by  $u, c, t, x$ , identifying the first three with the known quarks. Let  $u'_L, c'_L, t'_L$  be the three orthonormal linear combinations of left chiral components that form  $SU(2)_L$  doublets with the known  $Q = -\frac{1}{3}$  fields  $d_L, s_L, b_L$ , respectively, while the remaining combination  $x'_L$  is a singlet. We can then write

$$\begin{pmatrix} \bar{u}'_L & \bar{c}'_L & \bar{t}'_L & \bar{x}'_L \end{pmatrix} = \begin{pmatrix} \bar{u}_L & \bar{c}_L & \bar{t}_L & \bar{x}_L \end{pmatrix} \begin{pmatrix} \hat{V}_{ud} & \hat{V}_{us} & \hat{V}_{ub} & \hat{V}_{uo} \\ \hat{V}_{cd} & \hat{V}_{cs} & \hat{V}_{cb} & \hat{V}_{co} \\ \hat{V}_{td} & \hat{V}_{ts} & \hat{V}_{tb} & \hat{V}_{to} \\ \hat{V}_{xd} & \hat{V}_{xs} & \hat{V}_{xb} & \hat{V}_{xo} \end{pmatrix}. \quad (18)$$

The first three rows of the unitary matrix  $\hat{V}$  control the  $SU(2)_L$  couplings of  $W$  and  $Z$ ; the first three rows and columns of  $\hat{V}$  are precisely  $V_{CKM}$  (now generally non-unitary). The  $Z$



couplings to the  $SU(2)_L$  left-handed doublet and singlet weak eigenstates  $q'_L = u'_L, c'_L, t'_L, x'_L$  are given by

$$\mathcal{L} = g_Z \sum_{q'} \bar{q}'_L \left( -T_3 + \frac{2}{3} \sin^2 \theta_W \right) \gamma^\mu Z_\mu q'_L \quad (19)$$

and the FCNC couplings between mass eigenstates  $q_i = u, c, t, x$  are

$$\mathcal{L}_{\text{FCNC}} = -\frac{1}{2} g_Z \sum_{i \neq j} \hat{z}_{ij} \bar{q}_{iL} \gamma^\mu Z_\mu q_{jL} , \quad (20)$$

with

$$\hat{z}_{ij} = \hat{V}_{id} \hat{V}_{jd}^* + \hat{V}_{is} \hat{V}_{js}^* + \hat{V}_{ib} \hat{V}_{jb}^* = \delta_{ij} - \hat{V}_{io} \hat{V}_{jo}^* , \quad (21)$$

using the unitarity of  $\hat{V}$ . Here again the FCNC coefficients  $\hat{z}_{ij}$  are direct measures of non-unitarity in  $V_{CKM}$ . The corresponding FDNC couplings are

$$\mathcal{L}_{\text{FDNC}} = g_Z \sum_{i=u,c,t,x} \bar{q}_i \gamma^\mu Z_\mu \left[ -\frac{1}{4} \hat{z}_{ii} (1 - \gamma_5) + \frac{2}{3} \sin^2 \theta_W \right] q_i . \quad (22)$$

For standard  $u, c, t$  quarks, mixing with  $x$  again reduces left-handed FDNC and leaves right-handed FDNC unchanged.

The decay-width formulas are obtained from Eqs.(13)- (14), by substituting  $\hat{V}_{xi}$  and  $\hat{z}_{jx}$  for  $V_{ix}$  and  $z_{jx}$ .

(d) One  $Q = -\frac{1}{3}$  quark and one  $Q = \frac{2}{3}$  quark mixing

We here combine the notations of (b) and (c) above, and define

$$(\bar{u}'_L, \bar{c}'_L, \bar{t}'_L, \bar{x}'_{uL}) = (\bar{u}_L, \bar{c}_L, \bar{t}_L, \bar{x}_{uL}) \hat{V} \quad (23)$$

to be three doublet and one singlet  $Q = \frac{2}{3}$  fields, while

$$\begin{pmatrix} d'_L \\ s'_L \\ b'_L \\ x'_{dL} \end{pmatrix} = V \begin{pmatrix} d_L \\ s_L \\ b_L \\ x_{dL} \end{pmatrix} \quad (24)$$

are the corresponding three doublets (paired with  $u'_L, c'_L, t'_L$ ) and remaining singlet  $Q = -\frac{1}{3}$  fields. Neutral-current couplings of  $x_d$  and  $x_u$  are as in (b) and (c) above. Charged-current couplings are defined via the matrix  $\hat{V}\Delta V$ , where  $\Delta$  is diagonal with elements 1, 1, 1, 0 down the diagonal;  $\hat{V}\Delta V$  generalizes the CKM matrix, its first three rows and columns being simply  $V_{\text{CKM}}$ . For more general mixing parametrizations, see Refs. [18,20].

### III. $4 \times 4$ MIXING MATRIX

#### (a) Experimental constraints

When extra quarks are mixed in, unitarity constraints no longer apply to the  $3 \times 3$  CKM submatrix. Without these constraints, the CKM matrix elements lie in the following ranges [28]:

$$|V| = \begin{pmatrix} 0.9728 - 0.9757 & 0.218 - 0.224 & 0.002 - 0.005 & .. \\ 0.180 - 0.228 & 0.800 - 0.975 & 0.032 - 0.048 & .. \\ 0.0 - 0.013 & 0.0 - 0.56 & 0.0 - 0.9995 & .. \\ .. & .. & .. & .. \end{pmatrix} \quad (25)$$

However these numbers were obtained before the evidence for the top quark at Fermilab [29]. The presence of an apparent top quark signal in  $b$ -tagged events at, or even above, the predicted SM rate [29,30], strongly suggests a dominant  $t \rightarrow bW$  decay with  $|V_{tb}| \simeq 1$ . With this extra constraint, all the off-diagonal elements of the  $4 \times 4$  quark mixing matrix  $V$  (or  $\hat{V}$ ) are necessarily small. One can then generalize the Wolfenstein parameterization

$$V_{us} \sim \lambda, \quad V_{ub} \sim \lambda^3 A(\rho - i\eta), \quad V_{cb} \sim \lambda^2 A, \quad V_{td} \sim \lambda^3 A(1 - \rho - i\eta), \quad (26)$$

by taking for example (for the  $Q = -\frac{1}{3}$  case  $V$ )

$$V_{od} \sim B(\alpha - i\beta), \quad V_{os} \sim B(\sigma - i\tau), \quad V_{ob} \sim B. \quad (27)$$

Here the new parameters  $\alpha, \beta, \sigma, \tau, B$  are real and  $B$  is small (no hierarchy of these elements is imposed here). Often it is more convenient to adopt a parameterization in terms

of the sines  $s_i = \sin \theta_i$  of small angles  $\theta_i$ , setting  $\cos \theta_i \simeq 1$  and neglecting all  $s_i s_j$  terms except  $s_1 s_2$  (see also Ref. [22]):

$$V \simeq \begin{pmatrix} 1 & s_1 & s_3 e^{-i\delta_1} & s_6 \\ -s_1 & 1 & s_2 & s_5 e^{-i\delta_3} \\ -s_3 e^{i\delta_1} + s_1 s_2 & -s_2 & 1 & s_4 e^{-i\delta_2} \\ -s_6 & -s_5 e^{i\delta_3} & -s_4 e^{i\delta_2} & 1 \end{pmatrix}. \quad (28)$$

In this parameterization, the FCNC coefficients ( $z_{ij} = z_{ji}^*$ ) are

$$\begin{aligned} z_{ds} &= -s_5 s_6 e^{i\delta_3}, & z_{db} &= -s_4 s_6 e^{i\delta_2}, & z_{sb} &= -s_4 s_5 e^{i(\delta_2 - \delta_3)} \\ z_{dx} &= s_6, & z_{sx} &= s_5 e^{-i\delta_3}, & z_{bx} &= s_4 e^{-i\delta_2}. \end{aligned} \quad (29)$$

Similarly, if this parameterization is applied to  $\hat{V}$  in the case of one  $Q = \frac{2}{3}$  singlet quark, we have FCNC coefficients ( $\hat{z}_{ij} = \hat{z}_{ji}^*$ )

$$\begin{aligned} \hat{z}_{uc} &= -s_5 s_6 e^{i\delta_3}, & \hat{z}_{ut} &= -s_4 s_6 e^{i\delta_2}, & \hat{z}_{ct} &= -s_4 s_5 e^{i(\delta_2 - \delta_3)} \\ \hat{z}_{ux} &= -s_6, & \hat{z}_{cx} &= -s_5 e^{-i\delta_3}, & \hat{z}_{tx} &= -s_4 e^{-i\delta_2}. \end{aligned} \quad (30)$$

### (b) Unitarity constraints

Unitarity constraints on the  $3 \times 3$  CKM matrix give linear three-term relations that can be expressed graphically as triangle relations in the complex plane; see Fig. 1. With  $4 \times 4$  mixing, they become four-term relations; e.g. for one  $Q = -\frac{1}{3}$  singlet, we have

$$V_{ui}^* V_{uj} + V_{ci}^* V_{cj} + V_{ti}^* V_{tj} + V_{oi}^* V_{oj} = \delta_{ij}, \quad (31)$$

or again,

$$V_{id}^* V_{jd} + V_{is}^* V_{js} + V_{ib}^* V_{jb} + V_{ix}^* V_{jx} = \delta_{ij}. \quad (32)$$

For  $i \neq j$  these are expressible as quadrangle conditions in the complex plane. The first three terms in each case, however, are precisely the three sides of a triangle if CKM unitarity holds (the most discussed example is Eq.(31) with  $i = b, j = d$ ). Thus  $4 \times 4$  unitarity replaces the CKM triangle relations by quadrangle relations. In Eq.(31) the fourth side of the quadrangle

is  $V_{oi}^*V_{oj} = -z_{ij}$ , the FCNC coefficient [22]. In Eq.(32) the fourth side is  $V_{ix}^*V_{jx}$ , that occurs in certain flavor-changing box diagrams (see below).

In the case of one  $Q = -\frac{1}{3}$  singlet quark, the squares of the elements in each row and column of the  $4 \times 4$  unitary matrix  $V$  sum to unity. Hence the experimental lower bounds on the CKM submatrix elements [28] shown in Eq.(25) give constraints:

$$\begin{aligned} |V_{ux}| &\lesssim 0.08, & |V_{cx}| &\lesssim 0.57, & |V_{tx}| &\lesssim 1.0, \\ |V_{od}| &\lesssim 0.15, & |V_{os}| &\lesssim 0.56, & |V_{ob}| &\lesssim 1.0. \end{aligned} \quad (33)$$

Also each quadrangle must close, so the exotic fourth side is bounded by the sum of the upper limits of the three conventional CKM sides, giving

$$\begin{aligned} |V_{ux}||V_{cx}| &\lesssim 0.44, & |V_{ux}||V_{tx}| &\lesssim 0.15, & |V_{cx}||V_{tx}| &\lesssim 0.60, \\ |V_{od}||V_{os}| &\lesssim 0.45, & |V_{od}||V_{ob}| &\lesssim 0.03, & |V_{os}||V_{ob}| &\lesssim 0.61. \end{aligned} \quad (34)$$

Finally, when eventually we obtain upper bounds on  $|V_{oj}|$  ( $j = d, s, b$ ) from other data, unitarity will imply a lower bound on  $|V_{ox}|^2 = 1 - \sum_j |V_{oj}|^2$ , and hence an upper bound on  $\sum_i |V_{ix}|^2 = 1 - |V_{ox}|^2$ ; this latter bound will apply equally to each  $|V_{ix}|^2$  in the summation ( $i = u, c, t$ ). See Section VI(e) below.

In the case of one  $Q = \frac{2}{3}$  singlet quark, bounds on the CKM submatrix elements of the mixing matrix  $\hat{V}$  of Eq.(18) give analogous constraints:

$$\begin{aligned} |\hat{V}_{uo}| &\lesssim 0.08, & |\hat{V}_{co}| &\lesssim 0.57, & |\hat{V}_{to}| &\lesssim 1.0, \\ |\hat{V}_{xd}| &\lesssim 0.15, & |\hat{V}_{xs}| &\lesssim 0.56, & |\hat{V}_{xb}| &\lesssim 1.0, \\ |\hat{V}_{uo}||\hat{V}_{co}| &\lesssim 0.44, & |\hat{V}_{uo}||\hat{V}_{to}| &\lesssim 0.15, & |\hat{V}_{co}||\hat{V}_{to}| &\lesssim 0.60, \\ |\hat{V}_{xd}||\hat{V}_{xs}| &\lesssim 0.45, & |\hat{V}_{xd}||\hat{V}_{xb}| &\lesssim 0.03, & |\hat{V}_{xs}||\hat{V}_{xb}| &\lesssim 0.61. \end{aligned} \quad (35)$$

#### IV. DIRECT SINGLET-QUARK PRODUCTION CONSTRAINTS

##### (a) $Z$ decays

At  $e^+e^-$  colliders,  $\bar{x}x$  pairs can be produced directly via their  $\gamma$  and  $Z$  couplings, and  $x\bar{q}$  or  $\bar{x}q$  pairs via FCNC. The most stringent bounds at present come from the observed  $Z$  decay widths, from which it appears that contributions beyond the SM are limited by [31]

$$\Gamma_Z(\text{non-SM}) \lesssim 15 \text{ MeV} . \quad (36)$$

For the case  $Q_x = -\frac{1}{3}$ , the partial widths for decay to one light plus one new quark are

$$\Gamma(Z \rightarrow \bar{d}x) = \Gamma(Z \rightarrow d\bar{x}) = 3\Gamma_Z^0 K |z_{dx}|^2 F_x = (0.66 \text{ GeV}) |z_{dx}|^2 F_x, \quad (37)$$

and for the case  $Q_x = \frac{2}{3}$  we have

$$\Gamma(Z \rightarrow \bar{u}x) = \Gamma(Z \rightarrow u\bar{x}) = 3\Gamma_Z^0 K |\hat{z}_{ux}|^2 F_x = (0.66 \text{ GeV}) |\hat{z}_{ux}|^2 F_x, \quad (38)$$

where  $\Gamma_Z^0 = G_F M_Z^3 / (12\pi\sqrt{2}) = 0.17 \text{ GeV}$ ,  $F_x = (1 - m_x^2/M_Z^2)^2 (1 + m_x^2/2M_Z^2)$  and  $K = 1 + (8\pi/9)\alpha_s(M_Z) = 1.33$  is a QCD factor. For each  $x\bar{q} + \bar{x}q$  contribution to remain within the bound on  $\Gamma_Z(\text{non-SM})$  sets  $m_x$ -dependent constraints on the FCNC coefficients,

$$\sqrt{F_x} |z_{ix}| \lesssim 0.11 \quad i = d, s, b, \quad (Q_x = -\frac{1}{3}) \quad (39)$$

$$\sqrt{F_x} |\hat{z}_{jx}| \lesssim 0.11 \quad j = u, c, \quad (Q_x = \frac{2}{3}). \quad (40)$$

The partial widths for decays to  $\bar{x}x$  pairs are

$$\Gamma(Z \rightarrow \bar{x}x) = 24\Gamma_Z^0 K \left[1 - 4m_x^2/M_Z^2\right]^{1/2} \left[g_V^2(1 + 2m_x^2/M_Z^2) + g_A^2(1 - 4m_x^2/M_Z^2)\right] \quad (41)$$

where

$$g_V = -\frac{1}{4}z_{xx} + \frac{1}{3}\sin^2\theta_W, \quad g_A = -\frac{1}{4}z_{xx} \quad (Q_x = -\frac{1}{3}),$$

$$g_V = \frac{1}{4}\hat{z}_{xx} - \frac{2}{3}\sin^2\theta_W, \quad g_A = \frac{1}{4}\hat{z}_{xx} \quad (Q_x = \frac{2}{3}).$$

In the limit of small singlet-doublet mixing, we have  $z_{xx} \simeq 0$  or  $\hat{z}_{xx} \simeq 0$  and hence  $g_V \simeq -Q_x \sin^2\theta_W$ ,  $g_A \simeq 0$ . In this limit the upper bound  $\Gamma(Z \rightarrow \bar{x}x) < \Gamma_Z(\text{non-SM})$  gives

$$m_x \gtrsim 42 \text{ GeV} \quad (Q_x = -\frac{1}{3}), \quad (42)$$

$$m_x \gtrsim 45 \text{ GeV} \quad (Q_x = \frac{2}{3}). \quad (43)$$

Figure 2 shows the corresponding  $\bar{x}x$  contribution to  $\Gamma_Z(\text{non-SM})$  versus  $m_x$  for  $Q_x = -\frac{1}{3}$  and  $\frac{2}{3}$ . Direct searches at LEP for typical heavy quark signals ( $t \rightarrow bW^{*+}$ ,  $b' \rightarrow cW^{*-}$ ), based simply on event shapes, set early limits  $m_t > 44.5 \text{ GeV}$  and  $m_{b'} > 45.2 \text{ GeV}$  [32], corresponding to upper limits  $\Gamma(Z \rightarrow \bar{b}'b', \bar{t}t) < 20 - 30 \text{ MeV}$ . Applying these limits to

singlet quarks gives a weaker result than Eq.(42) and about the same as Eq.(43); some improvements could presumably be achieved with present much higher luminosities.

(b) Hadroproduction

At hadron colliders,  $\bar{x}x$  pairs can be produced via QCD interactions exactly like SM quark pairs. Their  $x \rightarrow q'W$  CC decays into lighter quarks give signals rather similar to the  $t \rightarrow bW$  signals that have been looked for in top-quark searches [29,30,33], although the details may differ; they also have new decays into  $qZ$  and/or  $qH$ . We briefly discuss some examples.

(i) For a heavy  $Q = \frac{2}{3}$  singlet  $x_t$  that mixes mostly with  $t$  and has  $M_W < m_{x_t} < M_W + m_t$ , the dominant decay mode is  $x_t \rightarrow bW$  while  $x_t \rightarrow tZ, tH$  are kinematically forbidden. Hence the  $\bar{x}_t x_t$  signals look *exactly* like  $\bar{t}t$  signals, including the presence of taggable  $b$ -jets in the final state. Lower bounds on  $m_t$  such as the D0 result [30]  $m_t > 131$  GeV apply also to  $m_{x_t}$ . Recently published evidence for  $t\bar{t}$  production [29] could in principle be interpreted as  $\bar{x}_t x_t$  production, but electroweak radiative corrections [34] already indicate a top mass near the observed value, making  $t\bar{t}$  production the most likely interpretation. However, if there is an excess of top-type events above the SM rate [29], this could be due to  $\bar{x}_t x_t$  production in addition to  $t\bar{t}$  production [16].

(ii) A  $Q = -\frac{1}{3}$  singlet  $x_b$  that mixes mostly with  $b$  and has  $M_Z < m_{x_b} < m_t + M_W$  would decay dominantly via  $x_b \rightarrow bZ, bH$  with the  $tW$  mode suppressed, escaping the usual top searches but offering new  $Z$  and  $H$  signals. If the latter are suppressed (e.g., if  $m_H > m_{x_b}$ ), early CDF limits on the remaining  $Z$  signals imply a bound  $m_{x_b} > 85$  GeV [13]. This scenario gains fresh interest [16] from hints of possible excess tagged  $Z$  plus four jet events at the Tevatron [29].

To be quantitative about signal expectations with  $b$ -tagging, let us consider  $x_b$  and  $t$  to be degenerate ( $m_{x_b} \simeq m_t$ ) for simplicity, so that they are produced equally. If  $x_b$  is lighter than this, the singlet signal rates will be correspondingly higher. For the singlet decay we consider two extreme scenarios: (A)  $m_H > m_{x_b} > M_Z$ , so that  $\Gamma(x_b \rightarrow bZ) \gg \Gamma(x_b \rightarrow bH)$

and (B)  $m_H \simeq M_Z$  with small  $b$ - $x_b$  mixing, so that  $\Gamma(x_b \rightarrow bZ) \simeq \Gamma(x_b \rightarrow bH)$ . For  $b$ -tagging efficiency, we assume  $\epsilon_b = 0.2$  to be the probability for tagging a single  $b$ -quark; then the probability for tagging a  $b\bar{b}$  event is  $1 - (1 - \epsilon_b)^2 = 0.36$  and the probability for tagging a  $b\bar{b}b\bar{b}$  event is  $1 - (1 - \epsilon_b)^4 = 0.59$ . Our discussion is simplified in that we neglect fake tags, assume  $b$ -tags are uncorrelated, and assume 100% acceptance. Then the probabilities for different final state configurations including  $b$ -tagging are

| <i>channel</i>                                      | <i>probability with tag</i> |
|---|-----------------------------|
| $\bar{b}bWW \rightarrow \bar{b}b(\ell\nu)(jj)$      | $0.29 \times 0.36 = 0.104$  |
| $\bar{b}bZZ \rightarrow \bar{b}b(\ell\ell)(jj, bb)$ | $0.094 \times 0.41 = 0.039$ |
| $\bar{b}bZH \rightarrow \bar{b}b(\ell\ell)(bb)$     | $0.067 \times 0.59 = 0.040$ |

summing over  $\ell = e, \mu$  channels. The first numerical factor on the right is the branching fraction and the second factor is the  $b$ -tagging probability. Thus the leptonic  $W/Z$  event ratios in our two  $m_{x_b} \simeq m_t$  scenarios (A) and (B) are

$$N(tt \rightarrow W_{\ell\nu} + 4j \text{ with tag})/N(xx \rightarrow Z_{\ell\ell} + 4j \text{ with tag}) \simeq 2.7(A) \quad \text{or} \quad 3.5(B). \quad (44)$$

In contrast, the QCD electroweak background ratio is [35]

$$N(QCD \rightarrow W_{\ell\nu} + 4j \text{ with tag})/N(QCD \rightarrow Z_{\ell\ell} + 4j \text{ with tag}) \simeq 10 - 14. \quad (45)$$

(iii) A  $Q = -\frac{1}{3}$  singlet quark  $x_d$  mixing mostly with  $d$  would decay by  $x \rightarrow uW, dZ, dH$  in the ratios  $2 : 1 : 1$  modulo phase space factors. Thus for  $m_x \gg M_W, M_Z, M_H$  the top-like signals would be reduced roughly by a factor 2 for single-lepton channels and by a factor 4 for dilepton signals, compared to a top quark of the same mass; however, for smaller  $m_x$  the reduction is generally less, and in the window  $M_W < m_x < M_Z, M_H$  there is no reduction. But there is now no  $b$ -quark to tag. Examination of earlier top-quark searches without a  $b$ -tag [30,33], scaling down the top-quark expectations by some factor between 1 and 4, shows that the range  $M_W < m_x < M_Z, M_H$  is definitely excluded, and probably some adjacent ranges of  $m_x$  too, but more cannot be said without detailed analysis. Similar conclusions apply to  $x_s$  singlets mixing mostly with  $s$  and to charge  $\frac{2}{3}$  singlets  $x_u$  or  $x_c$  mixing mostly

with  $u$  or  $c$ ; there are small differences between these cases, such as the lepton spectrum [10] and the taggability of  $c$ -quarks, but they do not change the overall conclusion.

(iv) Decays outside the detector. The distinctive  $x$ -quark signals will be lost if  $x$  decays outside the detector. If we assume typical Lorentz factors  $\beta\gamma \sim 2$  and require that the mean decay distance  $\ell_D = \beta\gamma c/\Gamma$  due to any single  $x \rightarrow q_i W, q_j Z$  decay mode exceeds one metre, Eqs.(13)-(14) give

$$|V_{ix}| \lesssim 1.2 \times 10^{-8} \left[ \frac{200 \text{ GeV}}{m_x} \right]^{\frac{3}{2}}, \quad |V_{oj}| \lesssim 0.9 \times 10^{-8} \left[ \frac{200 \text{ GeV}}{m_x} \right]^{\frac{3}{2}}, \quad (46)$$

for  $Q = -\frac{1}{3}$ , and similarly

$$|\hat{V}_{xi}| \lesssim 1.2 \times 10^{-8} \left[ \frac{200 \text{ GeV}}{m_x} \right]^{\frac{3}{2}}, \quad |\hat{V}_{oj}| \lesssim 0.9 \times 10^{-8} \left[ \frac{200 \text{ GeV}}{m_x} \right]^{\frac{3}{2}}, \quad (47)$$

for  $Q = \frac{2}{3}$ . If these conditions hold for all light quark flavors  $i, j$ , then singlet decay signals at hadron colliders will be greatly suppressed. [The conditions are somewhat weaker for  $m_x \lesssim M_W, M_Z$ ].

### (c) Leptoproduction

At  $ep$  colliders, singlet quarks can be produced by the same  $\gamma g$  fusion processes as SM quarks;  $Zg$  fusion is also possible (at reduced rates due to reduced  $Z\bar{x}x$  couplings) but  $Wg$  fusion is only possible via mixing. However, the reach of the HERA collider for new quark detection is much less than that of the Tevatron [36] so this is not a promising avenue for singlet discovery.

### (d) Summary

The LEP mass bounds Eqs.(42)-(43) are virtually unconditional. Hadroproduction bounds are much stronger in particular cases [e.g.  $m_x > 85 \text{ GeV}$  (131 GeV) if the decays  $x \rightarrow qZ$  ( $x \rightarrow qW$ ) dominate completely], but assume implicitly that the mixing with lighter quarks is not so extremely weak that  $x$  decays outside the detector [typified by off-diagonal 4th row and column mixing-matrix elements all being  $\lesssim 10^{-8}[(200 \text{ GeV})/m_x]^{\frac{3}{2}}$ ].



## V. NEUTRAL MESON-ANTIMESON OSCILLATIONS

The existence of new singlet quarks can affect neutral meson-antimeson oscillations in two different ways, through FCNC tree-level  $Z$  exchange and through box diagrams, illustrated in Fig. 3 for the  $B_d^0$ - $\bar{B}_d^0$  case. In the tree diagram of Fig. 3(a), the effects are due to an additional  $Q = -\frac{1}{3}$  singlet that generates the FCNC couplings of Eqs. (10)–(11); more generally, such FCNC effects of  $Q = -\frac{1}{3}$  singlets occur also for  $K^0$ - $\bar{K}^0$  and  $B_s^0$ - $\bar{B}_s^0$  oscillations, whereas analogous effects from  $Q = \frac{2}{3}$  singlets give  $D^0$ - $\bar{D}^0$  oscillations.

In the box diagram of Fig. 3(b), the effects come from an additional  $Q = \frac{2}{3}$  heavy quark option in the loop, along with corresponding reductions in the original three generation couplings. Similar effects are present in  $K^0$ - $\bar{K}^0$  and  $B_s^0$ - $\bar{B}_s^0$  oscillations, while analogous effects from  $Q = -\frac{1}{3}$  singlets occur in the  $D^0$ - $\bar{D}^0$  case. The association of singlets with their mixing effects is summarized in Table I.

### (a) $Z$ -exchange contributions

We first analyze the  $Z$ -exchange FCNC effects, which are potentially the most interesting. For  $B_d^0$ - $\bar{B}_d^0$  oscillations, the contribution is

$$|\delta m| = \frac{\sqrt{2}G_F m_B f_B^2 B_B \eta_B}{3} |z_{db}^2|, \quad (48)$$

where  $f_B$  is the  $B_d$  decay constant,  $B_B$  is the bag factor ( $B = 1$  is the vacuum saturation approximation) and  $\eta_B \approx 0.55$  is a QCD factor. (We assume the QCD correction is the same for both the  $Z$ -exchange contributions and for the box diagram contributions described below.) The analogous expressions for  $K^0$ - $\bar{K}^0$ ,  $D^0$ - $\bar{D}^0$ ,  $B_s^0$ - $\bar{B}_s^0$  oscillations involve  $Re(z_{ds}^2)$ ,  $\hat{z}_{uc}^2$ ,  $z_{sb}^2$ , respectively. Actually this FCNC process contributes coherently with the SM box diagrams. We shall here assume very conservatively that the singlet-quark  $Z$ -exchange contributions do not exceed the measured values. Then from the measurements [37]  $|\delta m|_K = (3.51 \pm 0.02) \times 10^{-12}$  MeV,  $|\delta m|_D < 1.3 \times 10^{-10}$  MeV,  $|\delta m|_{B_d} = (3.4 \pm 0.4) \times 10^{-10}$  MeV we obtain

$$|Re(z_{ds}^2)| = |(Re z_{ds})^2 - (Im z_{ds})^2| \lesssim 9 \times 10^{-8}, \quad (49)$$

$$|\hat{z}_{uc}| = |\hat{V}_{uo}| |\hat{V}_{co}| \lesssim 9 \times 10^{-4} , \quad (50)$$

$$|z_{db}| = |V_{od}| |V_{ob}| \lesssim 8 \times 10^{-4} , \quad (51)$$

where the  $\lesssim$  symbol reflects some uncertainties in the factors  $f$ ,  $B$ ,  $\eta$ . Similar bounds on  $z_{ds}$  and  $z_{db}$  are given in Ref. [18,22,25]) and on  $\hat{z}_{uc}$  in Ref. [26]. For  $|\delta m|_{B_s}$  there is only an experimental upper limit [37] and hence no bound on  $|z_{sb}| = |V_{os}| |V_{ob}|$ . We take the  $D$  and  $B$  decay constants from Narison [38]:  $f_D = 1.37 f_\pi$ ,  $f_B = 1.49 f_\pi$ , with  $f_\pi = 0.131$  GeV and  $f_K = 0.160$  GeV, and set  $B = 1$  and  $\eta = 0.55$  in all cases. Taking the lower bound  $B = \frac{1}{3}$  instead would raise the limits above by a factor  $\sqrt{3}$ .

### (b) New box diagram contributions

In the case of box diagram contributions, the constraints on the mixing are rather different. First consider the case of  $B_d^0$ - $\bar{B}_d^0$  box diagrams with an additional  $Q_x = \frac{2}{3}$  contribution, with  $m_x \simeq m_t$  approximate degeneracy. Then the SM formula is

$$|\delta m|_{\text{SM}} = \frac{G_F^2 B f_B^2 m_B \eta_B}{6\pi^2} |V_{td} V_{tb}^*|_{\text{CKM}}^2 |I_B| , \quad (52)$$

where  $I_B$  is a box-integral factor (see e.g. Ref. [39]), and the effect of adding an extra singlet is to replace the CKM factor by

$$\left| \hat{V}_{xd} \hat{V}_{xb}^* + \hat{V}_{td} \hat{V}_{tb}^* \right|^2 = |V_{ud} V_{ub}^* + V_{cd} V_{cb}^*|_{\text{CKM}}^2 \quad (53)$$

using unitarity. However,  $|V_{td} V_{tb}^*|_{\text{CKM}} = |V_{ud} V_{ub}^* + V_{cd} V_{cb}^*|_{\text{CKM}}$ , so the prediction for  $|\delta m|$  is effectively unchanged in this  $x, t$  mass-degenerate limit. Only if  $x$  is much heavier than  $t$  can significant changes arise. Similar conclusions apply to  $K^0$ - $\bar{K}^0$  oscillations.

The  $Q = -\frac{1}{3}$  box diagram contributions to  $D^0$ - $\bar{D}^0$  mixing are potentially more interesting, because  $d$ ,  $s$  and  $b$  are relatively light compared to the allowed mass scale for  $x$ . Here the  $x$  contributions may be dominant (depending on the size of the mixing) and given by

$$|\delta m|_D = \frac{G_F^2 B f_D^2 m_D \eta_D}{6\pi^2} |V_{cx} V_{ux}^*|^2 |I_D| , \quad (54)$$

where  $|I_D| \simeq m_x^2$  for  $m_x \sim 200$  GeV, giving

$$|V_{cx}| |V_{ux}| \lesssim 0.7 \times 10^{-2} \left( \frac{200 \text{ GeV}}{m_x} \right). \quad (55)$$

A similar bound is noted in Ref. [40] for mixing a fourth-generation  $b'$  quark, that is essentially equivalent to singlet mixing in this context. It is expected that a future sample of  $10^8$  reconstructed  $D$ 's would have a factor 20 improvement in sensitivity to  $\delta m_D$ , and would consequently give a factor  $\sim 4 - 5$  more sensitivity to the above mixing. Note that SM short- and long-distance contributions are far below this sensitivity [41,42].

The parameter  $\epsilon_K$ , that describes CP-violation in  $K^0 - \bar{K}^0$  oscillations, also receives tree-level  $Z$ -exchange contributions from  $Q = -\frac{1}{3}$  singlet mixing:

$$|\epsilon_K| = \frac{G_F m_K B_K f_K^2}{12 |\delta m_K|} |Im(z_{ds})^2|. \quad (56)$$

Requiring  $|\epsilon_K| \leq |\epsilon_K|_{exp} = 2.27 \times 10^{-3}$  gives the bound [22,25]

$$|Im(z_{ds})^2| \lesssim 6 \times 10^{-10}, \quad |Re(z_{ds}) Im(z_{ds})| \lesssim 3 \times 10^{-10}. \quad (57)$$

Combined with Eq.(49), this gives

$$|z_{ds}| = |V_{od}| |V_{os}| \lesssim 3 \times 10^{-4}. \quad (58)$$

## VI. FCNC DECAYS AND FDNC EFFECTS

### (a) $K_L \rightarrow \mu^+ \mu^-$ decay

Experimental measurements on FCNC decays imply constraints on the FCNC  $Z$  couplings and hence on singlet-quark mixing parameters [3,4,18,22,23]. For example,  $K_L \rightarrow \mu^+ \mu^-$  has a  $Z$ -mediated diagram if a  $Q = -\frac{1}{3}$  singlet  $x$  mixes with  $d$  and  $s$ , contributing the decay width

$$\Gamma(K_L \rightarrow \mu^+ \mu^-)_Z = \frac{2G_F^2 f_K^2 m_K m_\mu^2}{8\pi} [1 - 4m_\mu^2/m_K^2]^{1/2} [(\frac{1}{2} - \sin^2 \theta_W)^2 + (\sin^2 \theta_W)^2] |z_{ds}|^2. \quad (59)$$

After subtracting the contribution for the  $\gamma\gamma$  intermediate state (an imaginary decay amplitude), the latest Brookhaven results [43] indicate an upper limit  $B_{real} < 5.6 \times 10^{-10}$  (90%

CL) on the contribution to the branching fraction from the real part of the decay amplitude. Using this to bound the contribution from  $Re(z_{ds})$  we obtain

$$|Re(z_{ds})| \lesssim 0.64 \times 10^{-5}. \quad (60)$$

The combined bound on  $|z_{ds}|$  remains unchanged.

(b)  $B^0, D^0 \rightarrow \mu^+ \mu^-$  decays

Analogous formulas describe the tree-level contributions to  $D^0 \rightarrow \mu^+ \mu^-$  and  $B^0 \rightarrow \mu^+ \mu^-$  decays (without the factor 2 because  $D^0$  and  $B^0$  are not pure  $CP = -1$  states). Requiring that the  $Z$ -exchange contributions are within the experimental limits  $B(D^0 \rightarrow \mu^+ \mu^-) < 1.1 \times 10^{-5}$  and  $B(B^0 \rightarrow \mu^+ \mu^-) < 5.9 \times 10^{-6}$  [37], gives the constraints

$$|\hat{z}_{uc}| = |\hat{V}_{uo}| |\hat{V}_{co}| \lesssim 0.20, \quad (61)$$

$$|z_{db}| = |V_{od}| |V_{ob}| \lesssim 0.04, \quad (62)$$

much weaker than the oscillation bounds Eqs.(50)-(51).

(c)  $B, D \rightarrow X \ell^+ \ell^-$  decays

The rare decays  $B \rightarrow X \ell^+ \ell^-$  occur at tree level, via FCNC couplings  $z_{db}$  and  $z_{sb}$  which give

$$\frac{\Gamma(B \rightarrow \ell^+ \ell^- X)}{\Gamma(B \rightarrow \ell^+ \nu X)} = \left[ \left( \frac{1}{2} - \sin^2 \theta_W \right)^2 + \sin^4 \theta_W \right] \times \frac{|z_{db}|^2 + |z_{sb}|^2}{|V_{ub}|^2 + \rho |V_{cb}|^2}, \quad (63)$$

where  $\rho \simeq 0.5$  is a phase space factor;  $\rho = 1 - 8r^2 + 8r^6 - r^8 - 24r^4 \ln(r)$  with  $r = m_c/m_b = 0.316 \pm 0.013$ . Hence the experimental limit  $B(B \rightarrow X \mu^+ \mu^-) \leq 5.0 \times 10^{-5}$  gives the constraints [22,23]

$$|z_{db}| = |V_{ob}| |V_{od}| \lesssim 0.04 \times |V_{cb}| \lesssim 2 \times 10^{-3}, \quad (64)$$

$$|z_{sb}| = |V_{ob}| |V_{os}| \lesssim 0.04 \times |V_{cb}| \lesssim 2 \times 10^{-3}. \quad (65)$$

The first bound is competitive with that from  $B_d - \bar{B}_d$  oscillations in Eq.(51). Upper limits have recently been given for some  $D \rightarrow \mu^+ \mu^- + \text{hadrons}$  branching fractions [44], suggesting

an inclusive upper limit of order  $(1 - 2) \times 10^{-3}$  (although no explicit value is quoted); such a limit would however only give  $|\hat{z}_{uc}| \lesssim 0.2 - 0.3$ , possibly competitive with Eq. (61) but much weaker than Eq. (50).

(d)  $B \rightarrow s(d)\gamma$  decays

The rare decays  $B \rightarrow s(d)\gamma$  have also been considered [24,45]. In the SM they go via  $W$ -loop diagrams; adding a down-type singlet quark introduces new  $Z$ -loop diagrams, using the FCNC couplings  $z_{ij}$  ( $H$ -loops are usually negligible). These can be incorporated into the conventional analyses by adding their contributions into the coefficients of the effective operators of the magnetic and chromomagnetic moment couplings  $f_\gamma^{(1)}$  and  $f_g^{(1)}$  as described in Appendix A. The ratio of  $\Gamma(b \rightarrow q\gamma)$  (where  $q = d, s$ ) to the inclusive semileptonic decay width is then given by

$$\frac{\Gamma(b \rightarrow q\gamma)}{\Gamma(b \rightarrow ce\nu)} = \frac{6\alpha}{\pi\rho\lambda} \frac{|V_{tq}^*V_{tb}|^2}{|V_{cb}|^2} |c_7(m_b)|^2, \quad (66)$$

where  $\alpha$  is the electromagnetic coupling and

$$c_7(m_b) = \left[ \frac{\alpha_s(M_W)}{\alpha_s(m_b)} \right]^{16/23} \left\{ c_7(M_W) - \frac{8}{3} c_8(M_W) \left[ 1 - \left( \frac{\alpha_s(m_b)}{\alpha_s(M_W)} \right)^{2/23} \right] \right\} + \sum_{i=1}^8 h_i \left( \frac{\alpha_s(M_W)}{\alpha_s(m_b)} \right)^{a_i}. \quad (67)$$

The Wilson coefficients  $c_7$  and  $c_8$ , the coefficients  $h_i$ , and the exponents  $a_i$  from the  $8 \times 8$  anomalous dimension matrix [46] are given in Appendix A. The phase-space factor  $\rho$  is defined below Eq.(63) and the QCD correction factor  $\lambda$  for the semileptonic process is  $\lambda = 1 - \frac{2}{3}f(r, 0, 0)\alpha_s(m_b)/\pi$  with  $f(r, 0, 0) = 2.41$  [47]. We remark that the FCNC diagrams include not only  $Z$ -loops but also tree-level  $Z$ -exchanges between the  $b$ -quark and the spectator antiquark in a decaying  $B$ -meson, not commented upon in previous literature. However, these  $Z$ -exchanges are suppressed relative to  $Z$ -loops by factors  $f_B/m_B \sim 1/25$  in decay amplitudes [48], so we do not pursue them here.

In the SM one expects the ratio  $B(b \rightarrow d\gamma)/B(b \rightarrow s\gamma) \approx |V_{td}/V_{ts}|^2$ , since the QCD corrections largely cancel out. The additional FCNC terms are proportional to  $z_{qb}/(V_{tb}V_{tq}^*)$  in each case ( $q = d, s$ ), and it has been shown that [24]

$$\left| \frac{z_{db}}{V_{tb}V_{td}^*} \right| \leq 0.93, \quad \left| \frac{z_{sb}}{V_{tb}V_{ts}^*} \right| \leq 0.04. \quad (68)$$

These limits permit singlet quarks to have greater impact on the  $b \rightarrow d\gamma$  rate (e.g. if  $z_{db} \sim z_{sb}$ ). On the other hand, one expects from the general decoupling theorem [49] that  $z_{db}$  is much smaller than  $z_{sb}$ .

An up-type singlet quark can also be considered. Its contribution is the same as from a standard fourth generation, giving

$$\frac{\Gamma(b \rightarrow q\gamma)}{\Gamma(b \rightarrow ce\nu)} = \frac{6\alpha}{\pi\rho\lambda} \left( \frac{|\hat{V}_{tq}^* \hat{V}_{tb} c_7^t(m_b) + \hat{V}_{xq}^* \hat{V}_{xb} c_7^x(m_b)|^2}{|V_{cb}|^2} \right), \quad (69)$$

where the matching conditions for the relevant Wilson coefficients are again given in Appendix A. The major contributions to  $B(b \rightarrow q\gamma)$  are now the  $t$ - and  $x$ -quark loop terms in Eq.(69). Notice that  $\Gamma(b \rightarrow q\gamma)$  is the same as in the SM when  $m_x = m_t$ , for the same reason as in  $B_d^0\text{-}\bar{B}_d^0$  and  $K^0\text{-}\bar{K}^0$  oscillations above. But if  $m_x$  deviates significantly from  $m_t$ , an enhancement or suppression relative to the SM can be expected (as with a fourth generation [50]).

Figure 4 shows the  $b \rightarrow s\gamma$  rate versus  $m_x$  with various values of  $|\hat{V}_{xs}^* \hat{V}_{xb}|$ , for the SM plus one up-type singlet quark. We have assumed here that the phase of  $\hat{V}_{xs}^* \hat{V}_{xb}$  is the same as that of  $\hat{V}_{ts}^* \hat{V}_{tb}$  within a sign, so that deviations from the SM are maximized. We note incidentally that the unitarity constraint on  $|\hat{V}_{xd}||\hat{V}_{xb}|$  helps to guarantee that  $B(b \rightarrow d\gamma)$  with a  $u$ -type singlet remains close to the SM.

### (e) $Z$ decays

We turn now to FDNC effects. At tree level, introducing mixing with a singlet quark  $x$  simply reduces the left-handed coupling of a conventional quark  $i$  by a factor  $1 - |V_{oi}|^2/(1 - \frac{2}{3} \sin^2 \theta_W)$  (for charge  $Q_x = Q_i = -\frac{1}{3}$ ), or by a factor  $1 - |\hat{V}_{io}|^2/(1 - \frac{4}{3} \sin^2 \theta_W)$  (for charge  $Q_x = Q_i = \frac{2}{3}$ ), leaving right-handed couplings unchanged; see Eqs. (12),(20). We shall neglect singlet-mixing effects at one-loop level, where they are small corrections to small corrections.

The  $Z$  partial decay widths, branching fractions and asymmetry measurements directly

probe the FDNC  $Zqq$  couplings.  $Z \rightarrow b\bar{b}$  decay is an interesting case to consider, since there is at present some discrepancy between the LEP data [31] and the SM prediction for the ratio  $R_b = \Gamma(Z \rightarrow b\bar{b})/\Gamma(Z \rightarrow \text{hadrons})$ :

$$R_b(\text{LEP}) = 0.2202 \pm 0.0020, \quad R_b(\text{SM}) = 0.2156 \pm 0.0004. \quad (70)$$

Since  $b-x$  mixing reduces the  $Z \rightarrow b\bar{b}$  coupling, it would make the discrepancy worse. The decay width has the form

$$\Gamma(Z \rightarrow b\bar{b}) = \frac{\sqrt{2}G_F M_Z^3}{\pi} \beta \left( \beta^2 (g_A^b)^2 + \frac{3-\beta^2}{2} (g_V^b)^2 \right), \quad (71)$$

where  $\beta$  is the CM velocity and  $g_A^b$  and  $g_V^b$  are the axial and vector  $Zbb$  couplings, so down-type singlet mixing dilutes the tree-level contribution by a factor  $\approx (1 - 2.4|V_{ob}|^2)$ . It is inadvisable to derive a limit on  $V_{ob}$  from this result alone, however, since the SM itself is on the verge of being excluded. Many models with down-type singlets also give corrections to  $Z \rightarrow b\bar{b}$  from mixing  $Z$  with a new  $Z'$ ; these too are typically negative [21].

A global comparison of all FDNC effects with the latest LEP and SLC data leads to the following constraints (see final paper of Ref. [21]):

$$\begin{aligned} |V_{od}|^2 < 0.0023, & \quad |V_{os}|^2 < 0.0036, & \quad |V_{ob}|^2 < 0.0020, \\ |\hat{V}_{uo}|^2 < 0.0024, & \quad |\hat{V}_{co}|^2 < 0.0042, \end{aligned}$$

assuming at most one singlet quark mixes with each conventional quark. From these numbers, unitarity of  $V$  then gives

$$|V_{ox}| > 0.996, \quad |V_{qx}| < 0.089, \quad (q = u, c, t). \quad (72)$$

#### (f) Other FDNC effects

Singlet mixing could also change FDNC effects in neutrino scattering and atomic parity-violation measurements [20], but there appear to be no useful constraints from this quarter.

## VII. CP ASYMMETRIES

The amount of CP violation in the SM is measured by the size of the unitarity triangle in Fig. 1. How this CP violation shows up in decays is determined by the angles of the unitarity triangle(s), which appear as CP asymmetries in decays to CP eigenstates. The angles

$$\beta \equiv \arg\left(-\frac{V_{cd}V_{cb}^*}{V_{td}V_{tb}^*}\right), \quad \alpha \equiv \arg\left(-\frac{V_{td}V_{tb}^*}{V_{ud}V_{ub}^*}\right), \quad (73)$$

that characterize CP violation, are directly measurable in  $B_d$  decays with  $b \rightarrow c$  and  $b \rightarrow u$  respectively. The prototype processes for measuring  $\beta$  and  $\alpha$  are  $B_d \rightarrow \psi K_S$  and  $B_d \rightarrow \pi^+\pi^-$  respectively. [The angle  $\gamma \equiv \arg(-V_{ud}V_{ub}^*/V_{cd}V_{cb}^*)$  can be measured in the decay  $B_s \rightarrow \rho K_S$ , which will prove much harder at a  $B$  factory because of the small branching fraction and the possible contamination from penguin contributions.] Present information on the third generation couplings does not tell us much about the asymmetries. Future improved measurements of the CKM mixing angles will pin down the SM prediction more precisely. We find the biggest uncertainty in the SM asymmetries stems from the uncertainty in  $V_{ub}$ , a quantity ripe for better measurement at a  $B$ -factory.

We assume as usual that the asymmetries are dominated by the interference between two amplitudes, one of which is given by  $B_d^0$ - $\bar{B}_d^0$  oscillations with  $\Gamma_{12} \ll M_{12}$ . The time-dependent CP asymmetry in the decay of a  $B_d^0$  or  $\bar{B}_d^0$  into some final CP eigenstate  $f$  is

$$\frac{\Gamma(B_d^0(t) \rightarrow f) - \Gamma(\bar{B}_d^0(t) \rightarrow f)}{\Gamma(B_d^0(t) \rightarrow f) + \Gamma(\bar{B}_d^0(t) \rightarrow f)} = -\text{Im} \lambda(B_d \rightarrow f) \sin(\delta m t), \quad (74)$$

where  $\delta m$  is the (positive) difference in meson masses, the mesons states evolve from flavor eigenstates  $B_d^0$  and  $\bar{B}_d^0$  at a time  $t = 0$ , and  $\text{Im} \lambda(B_d \rightarrow f)$  is the time-independent asymmetry. The quantity  $\text{Im} \lambda(B_d \rightarrow f)$  is  $-\sin 2\beta$  and  $\sin 2\alpha$  for  $f = \psi K_S$  and  $f = \pi^+\pi^-$  respectively in the SM (we neglect possible penguin diagrams in the decay  $B_d^0 \rightarrow \pi^+\pi^-$ ).

We consider the allowed range for the Wolfenstein parameterization involving  $\rho$  and  $\eta$  recently given in Ref. [51]. The angles  $\alpha$  and  $\beta$  are easily related to  $\rho$  and  $\eta$  through the unitarity triangle in Fig. 1



$$\sin 2\alpha = \frac{2\eta(\eta^2 + \rho(\rho - 1))}{(\eta^2 + (1 - \rho)^2)(\eta^2 + \rho^2)} , \quad (75)$$

$$\sin 2\beta = \frac{2\eta(1 - \rho)}{\eta^2 + (1 - \rho)^2} . \quad (76)$$

In the presence of  $d$ -type singlet quarks the unitarity triangle becomes a quadrangle as described in Section III, and the CP asymmetries in  $B$  decays are altered from SM expectations. The deviations occur in two ways.

(1) The angles  $\beta$  and  $\alpha$  no longer have SM values, because the revised unitarity constraint yields different allowed ranges and more general phases for the CKM elements.

(2) There is an additional  $B_d - \bar{B}_d$  oscillation contribution from tree-level  $Z$ -mediated graphs.

The asymmetry expressions are modified to

$$\text{Im } \lambda(B_d \rightarrow \psi K_S) = -\sin(2\beta + \arg\Delta_{bd}) , \quad (77)$$

$$\text{Im } \lambda(B_d \rightarrow \pi^+ \pi^-) = \sin(2\alpha + \arg\Delta_{bd}) , \quad (78)$$

where [24]

$$\Delta_{bd} = 1 + r_d e^{2i\theta_{bd}} , \quad (79)$$

$$r_d = \frac{4\pi M_W^2 \sin^2 \theta_W}{\alpha I_B(x_t)} \left| \frac{z_{bd}}{V_{td} V_{tb}^*} \right|^2 \simeq 140 \left| \frac{z_{bd}}{V_{td} V_{tb}^*} \right|^2 , \quad (80)$$

$$\theta_{bd} = \arg \left[ \frac{z_{bd}}{V_{td} V_{tb}^*} \right] , \quad (81)$$

and  $I_B(x_t = m_t^2/M_W^2)$  is the box integral(see e.g. Ref. [39])

$$I_B(x_t) = \frac{1}{4} M_W^2 \left[ x_t \left( 1 + \frac{9}{1-x_t} - \frac{6}{(1-x_t)^2} \right) - \frac{6x_t^3}{(1-x_t)^3} \ln x_t \right] . \quad (82)$$

The contribution of  $z_{db}$  to the unitarity quadrangle can be described by a magnitude and a phase  $\theta_{bd}$  (relative to  $V_{td} V_{tb}^*$ ). This phase can take any value between 0 and  $2\pi$ , but the magnitude must be consistent with closure of the quadrangle. In Fig. 5 we show the asymmetry for the decay  $B_d \rightarrow \psi K_S$  for different values of the parameters [24]

$$\delta_d \equiv \left| \frac{z_{bd}}{V_{td} V_{tb}^*} \right| , \quad \theta_{bd} , \quad (83)$$

with the CKM angles, the top mass and the  $B$  lifetime fixed at their central values:  $|V_{ud}| = 0.9743$ ,  $|V_{cd}| = 0.204$ ,  $|V_{ub}| = 0.0035$ ,  $|V_{cb}| = 0.40$ ,  $m_t = 174$  GeV and  $\tau_B = 1.50$  ps. We take  $\sqrt{Bf_B^2} = 195$  MeV as we did previously, and use the next-to-leading order value for the QCD correction  $\eta_B = 0.55$  [52]. By taking the coherent sum of the contributions to  $B_d^0\text{-}\bar{B}_d^0$  mixing from Eqs. (48) and (52), and the the mixing parameter  $x_d = \delta m/\Gamma = 0.71$ , one can determine  $|V_{td}V_{tb}^*|$ . The shaded band in Fig. 5 indicates the allowed range in the SM for the asymmetry  $\text{Im} \lambda(B_d \rightarrow \psi K_S)$ .

The quantity  $\delta_d$  can be quite large, as indicated by Eq. (68), but Fig. 5 shows big effects even with much smaller  $\delta_d$ . One notices that the CP asymmetry  $\text{Im} \lambda(B_d \rightarrow \psi K_S)$  is negative in the SM, but with sufficiently large  $\delta_d$  one can obtain positive values [22,24]. The effect of singlet quarks on CP asymmetries can therefore be dramatic [22,24].

The CP asymmetry  $\text{Im} \lambda(B_d \rightarrow \pi^+\pi^-)$  is shown in Fig. 6 for various values of  $\delta_d$  and  $\theta_{bd}$ . Here the SM expectation covers the entire range, so merely measuring the sign of the CP asymmetry could not upset the SM. But given well-determined CKM elements, deviations from SM predictions could be significant and could provide evidence for singlet quarks.

## VIII. GUT SOURCES OF SINGLET QUARKS

### (a) Generalities

GUT models provide arguments for the existence of particles with exotic quantum numbers, but also impose restrictions upon them. In this Section, we explore the constraints on singlet-quark models implied by coupling-constant unification and perturbativity. Most of the examples we consider are supersymmetric models, and one must bear in mind that these models have extra contributions to the processes described above, so that the constraints obtained can be affected.

Singlet quarks considered alone do not introduce gauge (or gravitational) anomalies, but they spoil the successful gauge coupling unification of the minimal supersymmetric model (MSSM) if the singlets are below the GUT scale, since they change the running of the

$SU(3)$  and  $U(1)$  couplings but not the  $SU(2)$  coupling. For down-type singlets, this can be remedied by adding more fermions to fill out the  $\mathbf{5}$  and  $\mathbf{5}^*$  representations of  $SU(5)$  or the  $\mathbf{10}$  of  $SO(10)$ ; see the examples below.

For up-type singlets, however, it is harder to find a consistent scenario, if one believes that gauge coupling unification is due to a GUT symmetry and therefore wants to retain the desert between the GUT scale and the scale of the exotic fermions. The model of Barbieri and Hall [5] postulates that singlet quarks arise as supersymmetric partners (gauginos) of gauge bosons from a unification group that assigns a fourth color to leptons, so here the singlet with the right quantum numbers to mix with the top quark is not a matter fermion at all. We can introduce top-like singlets as matter fermions by assigning them to the adjoint representation of the GUT group. The smallest suitable representation of matter fermions is then the  $\mathbf{45}$  of  $SO(10)$ , or the  $\mathbf{78}$  of  $E_6$ . But these representations are too large; they destroy the asymptotic freedom of the strong coupling, and contain extra doublet quarks besides. Alternatively, in the context of  $SU(5)$ , we can introduce one up-type singlet quark by adding one extra light  $\mathbf{10}$  and one  $\mathbf{10}^*$  representation; these bring one extra vector-singlet lepton plus a vector-doublet of quarks too, and restore gauge unification with  $b_3 = 0$  at one-loop level. Two-loop effects become large, however, and large threshold corrections must be invoked to restore gauge coupling unification. Apart from this  $\mathbf{10} + \mathbf{10}^*$  scenario, there appears to be no simple way to arrive at a low-energy model with up-type singlet quarks from a desert GUT model.

### (b) One-loop evolution equations

The evolution equations for the gauge couplings at one loop can be written

$$\frac{dg_i}{dt} = \frac{b_i g_i^3}{16\pi^2} \quad , \quad \frac{d}{dt}[\alpha_i^{-1}] = -\frac{b_i}{2\pi} \quad , \quad (84)$$

with  $t = \ln(\mu/M_Z)$  the logarithmic scale and  $\alpha_i = g_i^2/(4\pi)$ . The SM particle content alone gives  $b_1 = 4\frac{1}{10}$ ,  $b_2 = -3\frac{1}{6}$ ,  $b_3 = -7$ . It is well known that this does not lead to gauge coupling unification; given  $\alpha_2^{-1}$ ,  $\alpha_1^{-1}$  evolves too fast compared to  $\alpha_3^{-1}$ . Simply adding singlet quarks makes things worse, however;  $\alpha_2^{-1}$  is unchanged,  $\alpha_1^{-1}$  evolves faster and  $\alpha_3^{-1}$  evolves more

slowly. Some different particle content is needed.

The MSSM, with additional supersymmetric particle content and two Higgs doublets, does give successful gauge coupling unification with the beta functions

$$b_1 = 2n_G + \frac{3}{5}n_H, \quad (85)$$

$$b_2 = 2n_G + n_H - 6, \quad (86)$$

$$b_3 = 2n_G - 9, \quad (87)$$

where  $n_G = 3$  is the number of light generations of matter and  $n_H = 1$  is the number of pairs of light Higgs doublets. In the presence of  $n_{x_u}$  up-type and  $n_{x_d}$  down-type singlet quarks, the beta functions are modified to

$$b_1 = 2n_G + \frac{3}{5}n_H + \frac{2}{5}n_{x_d} + \frac{8}{5}n_{x_u}, \quad (88)$$

$$b_2 = 2n_G + n_H - 6, \quad (89)$$

$$b_3 = 2n_G - 9 + n_{x_d} + n_{x_u}. \quad (90)$$

These singlet quark contributions upset the MSSM unification as shown in Fig. 7. However, unification can be restored by adding exotic fermions to fill out one or more representations of  $SU(5)$ . For example, in an  $E_6$  model the basic **27** representation has the decompositions  $\mathbf{16} + \mathbf{10} + \mathbf{1}$  in the  $SO(10)$  subgroup, which in turn are  $(\mathbf{10} + \mathbf{5}^* + \mathbf{1}) + (\mathbf{5} + \mathbf{5}^*) + \mathbf{1}$  in  $SU(5)$ . If the full **27** of fermions is light, the down-type quarks are supplemented by colorless doublets and singlets, giving

$$b_1 = 3n_G + \frac{3}{5}n_H, \quad (91)$$

$$b_2 = 3n_G + n_H - 6, \quad (92)$$

$$b_3 = 3n_G - 9. \quad (93)$$

where  $n_G$  is now the number of light generations of  $E_6$  matter, assuming that the light Higgses are external to the **27** representations. Thus all  $b_i$  are shifted by the same amount  $n_G$  from the MSSM case; all values of  $\alpha_i^{-1}(t)$  are shifted down by the same amount  $-b_i t n_G / (2\pi)$  and

unification is preserved. Note incidentally that with the usual three generations we now have  $b_3 = 0$  and the strong coupling ceases to run.

However, one usually assumes instead that the pair of Higgs doublets comes from the **27**, in which case the beta functions are

$$b_1 = 3n_G , \quad (94)$$

$$b_2 = 3n_G - 6 , \quad (95)$$

$$b_3 = 3n_G - 9 , \quad (96)$$

and the gauge coupling unification is again problematic. One solution would be to get back to the previous successful beta functions by adding two new particles with the quantum numbers of two Higgs doublets. Alternatively, we might have hoped that the two-loop contributions could rescue gauge coupling unification, since the gauge couplings are all larger than in the MSSM, making two-loop contributions more important. Unfortunately the sign of the two-loop term pushes the  $SU(3)$  coupling further away from the electroweak couplings. Nevertheless, this example shows that two-loop contributions could be important.

### (c) Two-loop evolution equations

At two-loop level, the evolution equations become

$$\frac{dg_i}{dt} = \frac{g_i}{16\pi^2} \left[ b_i g_i^2 + \frac{1}{16\pi^2} \sum_{j=1}^3 b_{ij} g_i^2 g_j^2 \right] , \quad (97)$$

where the one-loop beta functions are

$$b_1 = \frac{3}{2}n_{10} + \frac{1}{2}(n_{5^*} + n_{5^{*'}} + n_5) + \frac{3}{5}n_H , \quad (98)$$

$$b_2 = \frac{3}{2}n_{10} + \frac{1}{2}(n_{5^*} + n_{5^{*'}} + n_5) + n_H - 6 , \quad (99)$$

$$b_3 = \frac{3}{2}n_{10} + \frac{1}{2}(n_{5^*} + n_{5^{*'}} + n_5) - 9 , \quad (100)$$

for an arbitrary number of copies  $(n_{10}, n_{5^*}, n_{5^{*'}}, n_5)$  in the **10**, **5\***, **5'**, and **5** representations of  $SU(5)$ , and  $n_H$  light pairs of Higgs doublets (from a split representation) . The two-loop coefficients  $b_{ij}$  are listed in Appendix B. The model-dependent contributions from

the Yukawa couplings at two-loop order have been neglected. In the absence of split representations the entries are related by simple  $SU(3)$  and  $SU(2)$  group factors. The second  $\mathbf{5}^{*'} representation contains the multiplet  $(H, x_d^c)$  which may come from either the  $\mathbf{10}$  or the  $\mathbf{16}$  representation of  $SO(10)$ .$

For rank 5  $E_6$  models there is an extra  $U(1)$  that enters into the gauge coupling evolution equations at the two-loop level. There is a one-parameter family of extra  $U(1)$ 's orthogonal to  $U(1)_Y$ . Three popular models [53] are characterized as follows:

- (1) the  $SO(10)$  singlet fermion is inert, with respect to the extra  $U(1)$ .
- (2) the  $SU(5)$  singlet fermion in the  $\mathbf{16}$  of  $SO(10)$  is inert, and
- (3) the  $\mathbf{5}^*$  and  $\mathbf{5}^{*'}$  have exactly the same quantum numbers.

We label the  $U(1)$  quantum number of these models by  $Y'$ ,  $Y''$ , and  $Y'''$  respectively, and list the quantum numbers for the full  $\mathbf{27}$  of  $E_6$  in Table II. Notice that for the first model the  $\mathbf{16}$  of  $SO(10)$  decomposes as  $\mathbf{10} + \mathbf{5}^{*' + \mathbf{1}}$ . The first two models could actually arise from an  $SO(10)$  theory, since  $\text{Tr } Y$  vanishes across each  $SO(10)$  multiplet, while the third model is distinctively  $E_6$  (as are all the rest of the rank 5 models). In the last model it is natural for the entire  $\mathbf{27}$  to be light. [We note that the extra abelian groups are often referred to by the notation  $U(1)_\eta$ ,  $U(1)_\chi$  and  $U(1)_\psi$  [4]; the models (2) and (3) considered here then correspond to the extra group being  $U(1)_\chi$  and  $U(1)_\eta$  respectively, while the model (1) is a linear combination of  $U(1)_\chi$  and  $U(1)_\psi$ .] For these three models one obtains, in addition to the RGE coefficients  $b_i$  and  $b_{ij}$  already listed, the one-loop coefficients

$$b'_p = \frac{1}{4}n_{10} + \frac{1}{2}(n_{5^*} + n_5) + \frac{9}{8}n_{5^{*'}} + \frac{5}{8}n_N + \frac{13}{20}n_H, \quad (101)$$

$$b''_p = \frac{1}{4}n_{10} + \frac{9}{8}n_{5^*} + \frac{1}{2}(n_{5^{*'}} + n_5) + \frac{5}{8}n_{\nu_L^c} + \frac{2}{5}n_H, \quad (102)$$

$$b'''_p = \frac{2}{3}n_{10} + \frac{1}{12}(n_{5^*} + n_{5^{*'}}) + \frac{4}{3}n_5 + \frac{5}{12}(n_N + n_{\nu_L^c}) + \frac{17}{30}n_H, \quad (103)$$

and the two-loop contributions are listed in the Appendix B. We use the subscript  $p$  (for “prime”) to distinguish the  $U(1)'$ ,  $U(1)''$  and  $U(1)'''$  gauge couplings and their RGE coefficients. Here  $n_N$  and  $n_{\nu_L^c}$  are the number of light singlets with the quantum numbers given in Table II. In a general model with more than one  $U(1)$  factor, one must account for the

mixing between the  $U(1)$ 's in the renormalization group equations [54]. This complication does not arise if one considers only unification trajectories. In any event the practical effect of the extra  $U(1)$  on the evolution is small. The above equations have been derived for an arbitrary number of different representations of  $SU(5)$ , but split representations in the  $\mathbf{10}$  of  $SO(10)$  have been allowed for ( $\mathbf{10} \rightarrow \mathbf{5} + \mathbf{5}^* \rightarrow H + \overline{H}$ ), since they may be needed to achieve gauge coupling unification. The beta functions for  $U(1)'$  and  $U(1)''$  are related by  $n_{5^*} \leftrightarrow n_{5^{*'}}'$  and  $n_N \leftrightarrow n_{\nu_L^c}$ . One can also consider the continuous family of rank 5  $E_6$  models that include the three above, but as far as gauge coupling unifications is concerned they offer no new features.

An  $E_6$  model with three light generations would have  $n_{10} = n_{5^*} = n_{\nu_L^c} = n_5 = n_{5^{*'}}' = n_N = 3$  (from the usual decomposition of the  $\mathbf{27}$  representation). If only complete  $\mathbf{27}$  multiplets of  $E_6$  occur, the above coefficients become universal, namely

$$b_1 = b'_p = b''_p = b'''_p = 3n_G, \quad (104)$$

$$b_2 = 3n_G - 6, \quad (105)$$

$$b_3 = 3n_G - 9, \quad (106)$$

and

$$b'_{ij} = b''_{ij} = b'''_{ij} = \begin{pmatrix} 3 & 1 & 3 & 8 \\ 1 & 3 & 3 & 8 \\ 1 & 1 & 21 & 8 \\ 1 & 1 & 3 & 34 \end{pmatrix} n_G + \begin{pmatrix} 0 & & & \\ & 0 & & \\ & & -24 & \\ & & & -54 \end{pmatrix}. \quad (107)$$

#### (d) Specific scenarios

These results allow us to examine gauge unification with different numbers of light generations of exotic matter, with or without a pair of light Higgses from a split representation. We recall that the MSSM has  $n_{10} = n_{5^*} = 3$ ,  $n_5 = n_{5^{*'}}' = 0$  with  $n_H = 1$  (the distinction between the  $\mathbf{5}^*$  and  $\mathbf{5}^{*'}'$  is immaterial as far as  $SU(5)$  is concerned), and the Higgs contribution is vital for successful unification.

(i) Extensions of the MSSM. Adding just one or two generations of  $SO(10)$  **10**-plet matter ( $n_5 = n_{5^*} = 1$  and keeping  $n_H = 1$ ) yields successful gauge coupling unification as shown in Fig. 8. With three generations, however, the two-loop corrections threaten to spoil unification; they also make  $\alpha_3$  increase toward the GUT scale (although  $b_3 = 0$  at one-loop). On the other hand, one expects the low-energy threshold corrections to be more significant in this case [55], and ultimately the success of unification depends on the details of the low-energy spectrum. [Ref. [55] assumes that the  $SU(5)$  multiplets are degenerate at the GUT scale.]

(ii)  $E_6$  based models. Here one needs some split representation since otherwise the electroweak couplings do not run fast enough for successful unification. (Some attempts at  $E_6$  phenomenology have assumed that the Higgs pair comes from a complete light representation.) The two-loop contributions do not help since they tend to slow the running of the strong coupling constant, or even make it grow in the case where the one-loop beta function  $b_3$  is exactly zero (as happens for three generations of light  $E_6$  matter). Although asymptotic freedom is lost above the exotic fermion mass scale, this is not necessarily a problem for gauge coupling unification as long as the two-loop effects do not make  $\alpha_3$  nonperturbative below the GUT scale. One has gauge unification at the same scale as in the MSSM (neglecting threshold correction), with unification coupling  $\alpha_3(M_{\text{exotic}})$  still perturbative, though significantly larger than in the MSSM.

(iii)  $E_6$  models with  $n_G = 3$ . In all  $E_6$  models one expects  $\alpha_3$  to run more slowly than in the MSSM due to the extra matter in the **5** and **5'** representations, keeping  $\alpha_3$  bigger and making two-loop contributions more important. We find that the latter destroy unification if there are three light generations of  $E_6$  matter (very similar to the case in Fig. 8) even when an extra Higgs pair is included; there are model-dependent deviations from the curves in Fig. 8, due to the presence of the extra  $U(1)$ , but these are very small. Gauge coupling unification would require  $\alpha_3(M_Z)$  to be reduced below the MSSM prediction by about 15%. Unification could conceivably still be rescued by threshold corrections from large splittings in the  $SU(5)$  multiplets at low energy. With three complete generations excluding the Hig-



gses, the situation is much worse as shown in Fig. 9.

(iv)  $SU(5)$  models with an extra  $\mathbf{10}$  and  $\mathbf{10}^*$ . This case is similar to case (iii), since the beta function coefficients  $b_3$  and  $b_{33}$  are the same. Two-loop contributions to the RGE's become relatively more important, and gauge coupling unification becomes problematic without large threshold corrections.

We have followed a philosophy of preferring the least number of split representations possible. It is possible to make gauge coupling unification work without an intermediate scale far removed from the electroweak scale by relaxing this constraint. In fact, a non-supersymmetric left-right  $E_6$  model has been proposed recently [56] in which the  $SU(2)_R$  is broken at 1 TeV.

#### (e) Yukawa evolution

One can consider the evolution of Yukawa couplings in this new scenario where the QCD coupling does not run as rapidly as it does in the MSSM. For  $b_3 = 0$  one can immediately solve the one-loop renormalization group equations (neglecting the  $SU(2)$  and  $U(1)$  couplings which are small except near the GUT scale).

Consider the superpotential

$$W = \lambda_t H_{2,3} Q t^c + \lambda_b H_{1,3} Q b^c + \lambda_\tau H_{1,3} L \tau^c + \lambda_{S_i} S_3 H_{1,i} H_{2,i} + \lambda_{d_i} S_3 x_{d_i} x_{d_i}^c. \quad (108)$$

We define  $H_{1,3}$ ,  $H_{2,3}$  and  $S_3$  to be the linear combination of the Higgs doublets and singlets that acquire a vev. For the top Yukawa coupling one has (assuming that  $\lambda_b$  and  $\lambda_\tau$  can be neglected)

$$\frac{d\lambda_t}{dt} = \frac{\lambda_t}{16\pi^2} \left[ -\sum_i c_i g_i^2 - 3g_2^2 - \frac{16}{3}g_3^2 + 6\lambda_t^2 + \lambda_{S_3}^2 \right], \quad (109)$$

where  $g_i$  are the running  $U(1)$  gauge couplings (and hence contain some model dependence).

The new couplings that arise from the presence of an electroweak Higgs singlet  $S$  evolve as

$$\frac{d\lambda_{S_3}}{dt} = \frac{\lambda_{S_3}}{16\pi^2} \left[ -\sum_i d_i g_i^2 - 3g_2^2 + 3\lambda_t^2 + 4\lambda_{S_3}^2 + 3\sum_j \lambda_{d_j}^2 \right], \quad (110)$$

$$\frac{d\lambda_{S_i}}{dt} = \frac{\lambda_{S_i}}{16\pi^2} \left[ -\sum_i d_i g_i^2 - 3g_2^2 + 3\lambda_t^2 + 4\lambda_{S_i}^2 \right] \quad i \neq 3, \quad (111)$$

$$\frac{d\lambda_{d_i}}{dt} = \frac{\lambda_{d_i}}{16\pi^2} \left[ -\sum_i e_i g_i^2 - \frac{16}{3} g_3^2 + 2\lambda_s^2 + 2\lambda_{d_i}^2 + 3\sum_j \lambda_{d_j}^2 \right], \quad (112)$$

where  $c_i$ ,  $d_i$  and  $e_i$  are some (in general model-dependent) coefficients of the  $U(1)$  gauge couplings. We do not assume any  $SU(5)$  relation between  $\lambda_{S_i}$  and  $\lambda_{d_i}$ .

Since the gauge coupling values near the GUT scale are much larger than they are in the minimal supersymmetric model, one expects the top Yukawa coupling to be driven much faster to its fixed point value from below. The general result is that if singlet quarks are accompanied by other exotics fermions to fill out representations of  $SU(5)$ , then the top-quark is driven to its fixed point value ( $\lambda_t^2 \approx 8/9g_3^2$ ) over a wide range of values for the top quark GUT scale Yukawa; see Fig. 10. The presence of the coupling  $\lambda_S$  in the top quark coupling RGE could soften the attraction to the fixed point, but requiring it to remain perturbative up to the GUT scale prevents it from destroying the fixed point solution, as shown in the NMSSM model [57].

The linear combinations  $H_{1,3}$ ,  $H_{2,3}$  and  $S_3$  of Higgs fields acquire vevs  $v_2$ ,  $v_1$  and  $v_s$  and one defines  $\tan\beta = v_2/v_1$ . One gets the usual relations that one has in the MSSM model

$$\lambda_b(m_t) = \frac{\sqrt{2}m_b(m_b)}{\eta_b v \cos\beta}, \quad \lambda_\tau(m_t) = \frac{\sqrt{2}m_\tau(m_\tau)}{\eta_\tau v \cos\beta}, \quad \lambda_t(m_t) = \frac{\sqrt{2}m_t(m_t)}{v \sin\beta}, \quad (113)$$

in addition to mass relations for the squark singlets and exotic leptons

$$\lambda_{d_i} = \frac{m_{x_{d_i}}}{v_s}, \quad \lambda_{S_i} = \frac{m_{H_i}}{v_s}, \quad (114)$$

ignoring mixing.

The singlet quark Yukawa couplings  $\lambda_{d_i}$  also have infrared fixed points [58], essentially given by the condition

$$2\lambda_{d_3}^2 + 3\sum_j \lambda_{d_j}^2 = \frac{16}{3}g_3^2. \quad (115)$$

Unfortunately this does not yield a prediction for the singlet quark mass since the Higgs singlet vev is a priori unknown. At best one can obtain an upper limit on the ratio  $m_{x_d}/M_{Z'}$  [58]. When the singlet quark Yukawa is at its fixed point, it saturates this upper limit.

One can also consider the implications of bottom-tau unification in the context of these  $E_6$  models. The evolution of the Yukawa couplings is the same as it is for the MSSM,

$$\frac{dR_{b/\tau}}{dt} = \frac{R_{b/\tau}}{16\pi^2} \left[ -\frac{4}{3}g_1^2 - \frac{16}{3}g_3^2 + \lambda_t^2 + 3\lambda_b^2 - 3\lambda_\tau^2 \right]$$

where  $R_{b/\tau} \equiv \frac{\lambda_b}{\lambda_\tau}$ . However, we find that since the gauge couplings are larger over the entire range of scales between  $M_{GUT}$  and the electroweak scale, the Yukawa couplings have to be correspondingly larger to cancel off the contributions from the gauge couplings. In the MSSM, the top Yukawa is often forced into the infrared fixed point region. In the  $E_6$  model with three light generations, we find that there is no solution that gives an acceptable value for  $m_b$  [55].

## IX. CONCLUSIONS

Quark singlets offer an interesting example of physics beyond the SM. They mix with the ordinary fermions. They impact a wide variety of experimental measurements, as they generate tree-level FCNC's, introduce unitarity violation in the SM CKM matrix, influence neutral meson-antimeson oscillations, and modify CP asymmetries. These objects can be produced by strong, electromagnetic and weak-neutral-current interactions, and produce interesting decay signatures. Their masses must generally exceed  $\frac{1}{2}M_Z$ ; higher limits 85-131 GeV apply in certain particular scenarios (see Section IV).

We have collected the available bounds on singlet quark mixing; some have been updated; some, such as the  $B^0, D^0 \rightarrow \mu^+\mu^-$  and  $D \rightarrow \mu^+\mu^-X$  constraints and the unitarity implications of FDNC bounds, have not appeared explicitly before (see Sections III-VI). The present limits on the  $4 \times 4$  mixing matrix elements connecting one new singlet quark

to standard quarks may be summarized as follows.

| <u><math>Q = -\frac{1}{3}</math> case</u>    | <u>limit</u>                   | <u>origin</u>                       |
|--|--------------------------------|-------------------------------------|
| $ V_{od} $                                   | $\lesssim 0.048$               | global FDNC                         |
| $ V_{os} $                                   | $\lesssim 0.060$               | global FDNC                         |
| $ V_{ob} $                                   | $\lesssim 0.045$               | global FDNC                         |
| $ V_{ux} $                                   | $\lesssim 0.08$                | CKM + unitarity                     |
| $ V_{cx} $                                   | $\lesssim 0.09$                | FDNC + unitarity                    |
| $ V_{tx} $                                   | $\lesssim 0.09$                | FDNC + unitarity                    |
| $ V_{ox} $                                   | $\gtrsim 0.996$                | FDNC + unitarity                    |
| $ V_{os}  V_{od} $                           | $\lesssim 3 \times 10^{-4}$    | $\epsilon, \delta m_K(\text{tree})$ |
| $ V_{ob}  V_{od} $                           | $\lesssim 8 \times 10^{-4}$    | $\delta m_B(\text{tree})$           |
| $ V_{ob}  V_{os} $                           | $\lesssim 2 \times 10^{-3}$    | $B \rightarrow \ell^+ \ell^- X$     |
| $ V_{cx}  V_{ux} $                           | $\lesssim (1.3\text{GeV})/m_x$ | $\delta m_D(\text{box})$            |
| $ Re(V_{od}^* V_{os})  Im(V_{od}^* V_{os}) $ | $\lesssim 3 \times 10^{-10}$   | $\epsilon_K$                        |
| $ Re(V_{od}^* V_{os}) $                      | $\lesssim 7 \times 10^{-6}$    | $K_L \rightarrow \mu\mu$            |

| <u><math>Q = \frac{2}{3}</math> case</u> | <u>limit</u>                | <u>origin</u>             |
|--|-----------------------------|---------------------------|
| $ \hat{V}_{uo} $                         | $\lesssim 0.049$            | global FDNC               |
| $ \hat{V}_{co} $                         | $\lesssim 0.065$            | global FDNC               |
| $ \hat{V}_{to} $                         | $\lesssim 1.0$              | unitarity                 |
| $ \hat{V}_{xd} $                         | $\lesssim 0.15$             | CKM + unitarity           |
| $ \hat{V}_{xs} $                         | $\lesssim 0.56$             | CKM + unitarity           |
| $ \hat{V}_{xb} $                         | $\lesssim 1.0$              | unitarity                 |
| $ \hat{V}_{co}  \hat{V}_{uo} $           | $\lesssim 9 \times 10^{-4}$ | $\delta m_D(\text{tree})$ |
| $ \hat{V}_{xd}  \hat{V}_{xb} $           | $\lesssim 0.03$             | CKM + unitarity           |

We have discussed possible effects of singlet quarks on  $b \rightarrow d\gamma, s\gamma$  decays, and have illustrated how a  $u$ -type singlet could either increase or decrease the SM rate for  $b \rightarrow s\gamma$  (Fig.4). We have pointed out that small  $x - q$  mixing reduces the branching fraction for

$Z \rightarrow q\bar{q}$  decays; in the interesting case  $Z \rightarrow b\bar{b}$ , this would worsen the present discrepancy between SM and experiment. We have given new illustrations of ways that singlet quarks can cause substantial deviations from SM expectations for CP-asymmetries of neutral  $B$  decays (Figs.5-6). The asymmetry  $\text{Im } \lambda(B_d \rightarrow \psi K_S)$  can have the opposite sign to the SM value.

In the GUT context, singlet quarks cannot simply be added by themselves to the SM or MSSM, since this would destroy gauge coupling unification (Fig.7); they must be accompanied by other members of exotic fermion multiplets. Down-type singlet quarks are readily accommodated in grand unified extensions of the SM; as a minimal scenario, they can be realized by adding one or more extra generations of  $\mathbf{5}$  and  $\mathbf{5}^*$  representations of  $SU(5)$ , that imply extra vector-doublet leptons too. This exotic matter together with the SM matter content fits into the  $\mathbf{27}$  representation of  $E_6$  (which decomposes to  $\mathbf{10} + \mathbf{5}^* + \mathbf{1} + \mathbf{5} + \mathbf{5}^* + \mathbf{1}$  in an  $SU(5)$  subgroup). Adding extra complete multiplets of  $SU(5)$  preserves (at the one-loop level) the successful unification of gauge couplings in the MSSM, since a complete multiplet contributes equally to the evolution of each coupling. However, more than three generations of exotic matter will destroy asymptotic freedom for  $\alpha_3$  at one loop (Fig.8).

As in the MSSM, gauge coupling unification in a desert model can be achieved by assuming that split representations exist. In the context of models with singlet quarks, this means that there must be an additional pair of light Higgs doublets, in addition to the pairs that are included with the singlet quarks in the  $\mathbf{5}$  and  $\mathbf{5}^*$  representations. (The MSSM is then a special case consisting of no singlet quarks and one light pair of Higgs doublets).

An up-type singlet quark is not contained as elegantly in GUT Models; it does not appear in the smallest representations, and its role is less clear. As a minimal prescription, it can be introduced by adding one extra light  $\mathbf{10}$  and one  $\mathbf{10}^*$  representation of  $SU(5)$  that get their mass from an  $SU(5)$  singlet Higgs boson; this implies extra vector-doublet quarks and a vector-singlet charged lepton too, preserving MSSM gauge coupling unification with  $b_3 = 0$  at one loop (Fig.8). Less minimally, it can also be realized in the  $SO(10)$  group with an extra light  $\mathbf{45}$  (adjoint) representation (which decomposes to  $\mathbf{24} + \mathbf{10}^* + \mathbf{10} + \mathbf{1}$  in an  $SU(5)$

subgroup), but this leads to nonperturbative gauge couplings at the GUT scale if the entire **45** is required to be light.

Two-loop effects are typically small in most GUT models, but if one includes extra representations of matter then the evolution of the strong coupling is diminished and it might even increase (no asymptotic freedom) toward the GUT scale. In a situation where the strong gauge coupling does not evolve at the one-loop level, we find that the two-loop effects become relatively more important and can make gauge coupling unification problematic, e.g. for three complete generations of  $E_6$  **27**-plet matter. However one expects the low-energy threshold corrections to be more significant in this case, and ultimately the success of unification depends on the details of the low-energy spectrum. Two-loop effects also threaten perturbativity and asymptotic freedom of  $\alpha_3$  (Figs.8-9).

Fixed points play a role in these extended model, with the top quark and the down-type singlet(s) masses possibly determined by the gauge couplings and the associated vevs. With extended matter content and larger gauge couplings, the top Yukawa coupling is driven to its fixed point faster than before (Fig.10). However, the Yukawa unification condition  $\lambda_b(M_G) = \lambda_\tau(M_G)$  becomes harder to accomodate, and fails in the  $E_6$  model with three light generations.

## X. APPENDIX A

In this appendix we collect a few results needed for the analysis of  $b \rightarrow q\gamma$  ( $q = s, d$ ) in Section VI. The SM magnetic and chromomagnetic couplings for flavor-changing  $b \rightarrow q$  decays via  $W$  loops are given by [59]

$$f_\gamma^{(1)} = \frac{7 - 5x - 8x^2}{36(x-1)^3} + \frac{x(3x-2)}{6(x-1)^4} \ln x, \quad (116)$$

$$f_g^{(1)} = \frac{2 + 5x - x^2}{12(x-1)^3} - \frac{x}{2(x-1)^4} \ln x, \quad (117)$$

where  $x = m_t^2/M_W^2$ . A down-type singlet quark induces additional  $Z$  loops, giving the replacements

$$\frac{3}{2}x f_\gamma^{(1)} \rightarrow \frac{3}{2}x f_\gamma^{(1)} + \left( \frac{z_{qb}}{V_{tb}V_{tq}^*} \right) \left( \frac{19}{54} - \frac{2}{81} \sin^2 \theta_W \right) , \quad (118)$$

$$\frac{3}{2}x f_g^{(1)} \rightarrow \frac{3}{2}x f_g^{(1)} + \left( \frac{z_{qb}}{V_{tb}V_{tq}^*} \right) \left( \frac{4}{9} + \frac{2}{27} \sin^2 \theta_W \right) . \quad (119)$$

These substitutions then enter into the values of the Wilson coefficients where

$$c_7(M_W) = \left[ \frac{3}{2}x f_\gamma^{(1)}(x) + \left( \frac{z_{qb}}{V_{tb}V_{tq}^*} \right) \left( \frac{19}{54} - \frac{2}{81} \sin^2 \theta_W \right) \right] , \quad (120)$$

$$c_8(M_W) = \left[ \frac{3}{2}x f_g^{(1)}(x) + \left( \frac{z_{qb}}{V_{tb}V_{tq}^*} \right) \left( \frac{4}{9} + \frac{2}{27} \sin^2 \theta_W \right) \right] . \quad (121)$$

The coefficients from the  $8 \times 8$  anomalous dimension matrix are [46]

$$a_i = \left( \frac{14}{23}, \quad \frac{16}{23}, \quad \frac{6}{23}, \quad -\frac{12}{23}, \quad 0.4086, \quad -0.4230, \quad -0.8994, \quad 0.1456 \right) \quad (122)$$

$$h_i = \left( \frac{626126}{272277}, \quad -\frac{56281}{51730}, \quad -\frac{3}{7}, \quad -\frac{1}{14}, \quad -0.6494, \quad -0.0380, \quad -0.0186, \quad -0.0057 \right)$$

In the case of up-type singlet quarks the Wilson coefficients are

$$c_7^t(M_W) = \frac{3}{2}x f_\gamma^{(1)}(x) , \quad (123)$$

$$c_7^x(M_W) = \frac{3}{2}y f_\gamma^{(1)}(y) , \quad (124)$$

$$c_8^t(M_W) = \frac{3}{2}x f_g^{(1)}(x) , \quad (125)$$

$$c_8^x(M_W) = \frac{3}{2}y f_g^{(1)}(y) , \quad (126)$$

where  $y = m_{x_u}^2/M_W^2$ .

## XI. APPENDIX B

We here collect some two-loop results needed in Section VIII. The two-loop RGE coefficients for an arbitrary number of  $\mathbf{10}$ ,  $\mathbf{5}^*$ , and  $\mathbf{5}$  representations are

$$b_{11} = \frac{23}{10}n_{10} + \frac{7}{30}(n_{5^*} + n_{5^{*'}} + n_5) + \frac{9}{25}n_H , \quad (127a)$$

$$b_{12} = \frac{3}{10}n_{10} + \frac{9}{10}(n_{5^*} + n_{5^{*'}} + n_5) + \frac{9}{5}n_H , \quad (127b)$$

$$b_{13} = \frac{24}{5}n_{10} + \frac{16}{15}(n_{5^*} + n_{5^{*'}} + n_5) , \quad (127c)$$

$$b_{21} = \frac{1}{10}n_{10} + \frac{3}{10}(n_{5^*} + n_{5^{*'}} + n_5) + \frac{3}{5}n_H, \quad (127d)$$

$$b_{22} = \frac{21}{2}n_{10} + \frac{7}{2}(n_{5^*} + n_{5^{*'}} + n_5) + 7n_H - 24, \quad (127e)$$

$$b_{23} = 8n_{10}, \quad (127f)$$

$$b_{31} = \frac{3}{5}n_{10} + \frac{2}{15}(n_{5^*} + n_{5^{*'}} + n_5), \quad (127g)$$

$$b_{32} = 3n_{10}, \quad (127h)$$

$$b_{33} = 17n_{10} + \frac{17}{3}(n_{5^*} + n_{5^{*'}} + n_5) - 54, \quad (127i)$$

in the  $g_1, g_2, g_3$  basis.

The two-loop coefficients for the  $E_6$  models are

$$b'_{pp} = \frac{1}{40}n_{10} + \frac{1}{5}(n_{5^*} + n_5) + \frac{81}{80}n_{5^{*'}} + \frac{25}{16}n_N + \frac{97}{200}n_H, \quad (128a)$$

$$b'_{p2} = \frac{3}{20}n_{10} + \frac{1}{5}(n_{5^*} + n_5) + \frac{9}{20}n_{5^{*'}} + \frac{39}{100}n_H, \quad (128b)$$

$$b'_{p3} = \frac{9}{20}n_{10} + \frac{3}{5}(n_{5^*} + n_5) + \frac{27}{20}n_{5^{*'}} + \frac{39}{20}n_H, \quad (128c)$$

$$b'_{p4} = \frac{6}{5}n_{10} + \frac{8}{5}(n_{5^*} + n_5) + \frac{18}{5}n_{5^{*'}}, \quad (128d)$$

$$b'_{1p} = \frac{3}{20}n_{10} + \frac{1}{5}(n_{5^*} + n_5) + \frac{9}{20}n_{5^{*'}} + \frac{39}{100}n_H, \quad (128e)$$

$$b'_{11} = \frac{23}{10}n_{10} + \frac{7}{30}(n_{5^*} + n_{5^{*'}} + n_5) + \frac{9}{25}n_H, \quad (128f)$$

$$b'_{12} = \frac{3}{10}n_{10} + \frac{9}{10}(n_{5^*} + n_{5^{*'}} + n_5) + \frac{9}{5}n_H, \quad (128g)$$

$$b'_{13} = \frac{24}{5}n_{10} + \frac{16}{15}(n_{5^*} + n_{5^{*'}} + n_5), \quad (128h)$$

$$b'_{2p} = \frac{3}{20}n_{10} + \frac{1}{5}(n_{5^*} + n_5) + \frac{9}{20}n_{5^{*'}} + \frac{13}{20}n_H, \quad (128i)$$

$$b'_{21} = \frac{1}{10}n_{10} + \frac{3}{10}(n_{5^*} + n_{5^{*'}} + n_5) + \frac{3}{5}n_H, \quad (128j)$$

$$b'_{22} = \frac{21}{2}n_{10} + \frac{7}{2}(n_{5^*} + n_{5^{*'}} + n_5) - 24, \quad (128k)$$

$$b'_{23} = 8n_{10}, \quad (128l)$$

$$b'_{3p} = \frac{3}{20}n_{10} + \frac{1}{5}(n_{5^*} + n_5) + \frac{9}{20}n_{5^{*'}}, \quad (128m)$$

$$b'_{31} = \frac{3}{5}n_{10} + \frac{2}{15}(n_{5^*} + n_{5^{*'}} + n_5), \quad (128n)$$

$$b'_{32} = 3n_{10}, \quad (128o)$$

$$b'_{33} = 17n_{10} + \frac{17}{3}(n_{5^*} + n_{5^{*'}} + n_5) - 54, \quad (128p)$$



$$b''_{pp} = \frac{1}{40}n_{10} + \frac{81}{80}n_{5^*} + \frac{1}{5}(n_{5^{*'}} + n_5) + \frac{25}{16}n_{\nu_L^c} + \frac{97}{200}n_H , \quad (129a)$$

$$b''_{p1} = \frac{3}{20}n_{10} + \frac{9}{20}n_{5^*} + \frac{1}{5}(n_{5^{*'}} + n_5) + \frac{6}{25}n_H , \quad (129b)$$

$$b''_{p2} = \frac{9}{20}n_{10} + \frac{27}{20}n_{5^*} + \frac{3}{5}(n_{5^{*'}} + n_5) + \frac{39}{20}n_H , \quad (129c)$$

$$b''_{p3} = \frac{6}{5}n_{10} + \frac{18}{5}n_{5^*} + \frac{8}{5}(n_{5^{*'}} + n_5) , \quad (129d)$$

$$b''_{p4} = \frac{3}{20}n_{10} + \frac{9}{20}n_{5^*} + \frac{1}{5}(n_{5^{*'}} + n_5) + \frac{6}{25}n_H , \quad (129e)$$

$$b''_{11} = \frac{23}{10}n_{10} + \frac{7}{30}(n_{5^*} + n_{5^{*'}} + n_5) + \frac{9}{25}n_H , \quad (129f)$$

$$b''_{12} = \frac{3}{10}n_{10} + \frac{9}{10}(n_{5^*} + n_{5^{*'}} + n_5) + \frac{9}{5}n_H , \quad (129g)$$

$$b''_{13} = \frac{24}{5}n_{10} + \frac{16}{15}(n_{5^*} + n_{5^{*'}} + n_5) , \quad (129h)$$

$$b''_{2p} = \frac{3}{20}n_{10} + \frac{9}{20}n_{5^*} + \frac{1}{5}(n_{5^{*'}} + n_5) + \frac{13}{20}n_H , \quad (129i)$$

$$b''_{21} = \frac{1}{10}n_{10} + \frac{3}{10}(n_{5^*} + n_{5^{*'}} + n_5) + \frac{3}{5}n_H , \quad (129j)$$

$$b''_{22} = \frac{21}{2}n_{10} + \frac{7}{2}(n_{5^*} + n_{5^{*'}} + n_5) - 24 , \quad (129k)$$

$$b''_{23} = 8n_{10} , \quad (129l)$$

$$b''_{3p} = \frac{3}{20}n_{10} + \frac{9}{20}n_{5^*} + \frac{1}{5}(n_{5^{*'}} + n_5) , \quad (129m)$$

$$b''_{31} = \frac{3}{5}n_{10} + \frac{2}{15}(n_{5^*} + n_{5^{*'}} + n_5) , \quad (129n)$$

$$b''_{32} = 3n_{10} , \quad (129o)$$

$$b''_{33} = 17n_{10} + \frac{17}{3}(n_{5^*} + n_{5^{*'}} + n_5) - 54 , \quad (129p)$$

$$b'''_{pp} = \frac{8}{45}n_{10} + \frac{1}{180}(n_{5^*} + n_{5^{*'}}) + \frac{64}{45}n_5 + \frac{25}{36}(n_N + n_{\nu_L^c}) + \frac{257}{450}n_H , \quad (130a)$$

$$b'''_{p1} = \frac{2}{5}n_{10} + \frac{1}{30}(n_{5^*} + n_{5^{*'}}) + \frac{8}{15}n_5 + \frac{17}{50}n_H , \quad (130b)$$

$$b'''_{p2} = \frac{6}{5}n_{10} + \frac{1}{10}(n_{5^*} + n_{5^{*'}}) + \frac{8}{5}n_5 + \frac{17}{10}n_H , \quad (130c)$$

$$b'''_{p3} = \frac{16}{5}n_{10} + \frac{4}{15}(n_{5^*} + n_{5^{*'}}) + \frac{64}{15}n_5 , \quad (130d)$$

$$b'''_{1p} = \frac{2}{5}n_{10} + \frac{1}{30}(n_{5^*} + n_{5^{*'}}) + \frac{8}{15}n_5 + \frac{17}{50}n_H , \quad (130e)$$

$$b'''_{11} = \frac{23}{10}n_{10} + \frac{7}{30}(n_{5^*} + n_{5^{*'}} + n_5) + \frac{9}{25}n_H, \quad (130f)$$

$$b'''_{12} = \frac{3}{10}n_{10} + \frac{9}{10}(n_{5^*} + n_{5^{*'}} + n_5) + \frac{9}{5}n_H, \quad (130g)$$

$$b'''_{13} = \frac{24}{5}n_{10} + \frac{16}{15}(n_{5^*} + n_{5^{*'}} + n_5), \quad (130h)$$

$$b'''_{2p} = \frac{2}{5}n_{10} + \frac{1}{30}(n_{5^*} + n_{5^{*'}}) + \frac{8}{15}n_5 + \frac{17}{30}n_H, \quad (130i)$$

$$b'''_{21} = \frac{1}{10}n_{10} + \frac{3}{10}(n_{5^*} + n_{5^{*'}} + n_5) + \frac{3}{5}n_H, \quad (130j)$$

$$b'''_{22} = \frac{21}{2}n_{10} + \frac{7}{2}(n_{5^*} + n_{5^{*'}} + n_5) - 24, \quad (130k)$$

$$b'''_{23} = 8n_{10}, \quad (130l)$$

$$b'''_{3p} = \frac{2}{5}n_{10} + \frac{1}{30}(n_{5^*} + n_{5^{*'}}) + \frac{8}{15}n_5, \quad (130m)$$

$$b'''_{31} = \frac{3}{5}n_{10} + \frac{2}{15}(n_{5^*} + n_{5^{*'}} + n_5), \quad (130n)$$

$$b'''_{32} = 3n_{10}, \quad (130o)$$

$$b'''_{33} = 17n_{10} + \frac{17}{3}(n_{5^*} + n_{5^{*'}} + n_5) - 54. \quad (130p)$$

## REFERENCES

- [1] V. Barger and S. Pakvasa, Phys. Lett. **81B**, 195 (1979); G.L. Kane and M. Peskin, Nucl Phys. **B195**, 29 (1982).
- [2] J.L. Rosner, Comm.Nucl.Part.Phys. **15**, 195 (1986).
- [3] V. Barger, N.G. Deshpande, R.J.N. Phillips and K. Whisnant, Phys. Rev. **D33**, 1912 (1986); V. Barger, R.J.N. Phillips and K. Whisnant, Phys. Rev. Lett. **57**, 48 (1986).
- [4] T.G. Rizzo, Phys. Rev. **D34**, 1438 (1986); J.L. Hewett and T.G. Rizzo, Z. Phys. **C34**, 49 (1987); Phys. Rep. **183**, 193 (1989).
- [5] R. Barbieri and L. Hall, Nucl. Phys. **B319**, 1 (1989).
- [6] E. Ma, Phys. Lett. **B322**, 363 (1994).
- [7] F. del Aguila, E. Laermann and P. Zerwas, Nucl. Phys. **B297**, 1 (1988);
- [8] F. del Aguila, G.L. Kane and M. Quiros, Phys. Rev. Lett. **63**, 942 (1989); F. del Aguila, Ll. Ametller, G.L. Kane and J. Vidal, Nucl. Phys. **B334**, 1 (1990).
- [9] V. Barger and K. Whisnant, Phys. Rev. **D41**, 2120 (1990).
- [10] V. Barger and R.J.N. Phillips, Phys. Rev. **D41**, 52 (1990).
- [11] P. Agrawal, S.D. Ellis and W.-S. Hou, Phys. Lett. **B256**, 289 (1991); W.-S. Hou, Phys. Rev. Lett. **69**, 3587 (1992).
- [12] B. Mukhopadhyaya, Phys. Rev. **D44**, R15 (1991); B. Mukhopadhyaya and S. Nandi, Phys. Rev. Lett. **66**, 285 (1991), *ibid.* **69**, 3588 (1992), Phys. Rev. **D46**, 5098 (1992).
- [13] D.P. Roy and B. Mukhopadhyaya, Phys. Rev. **D48**, 2105 (1993).
- [14] W.-S. Hou, Phys. Rev. Lett. **72**, 3945 (1994); W.S. Hou and H.-C. Huang, preprint MTUTH-94-18.
- [15] V. Barger and E. Ma, Phys. Rev. **D51**, 1332 (1995).

- [16] V. Barger and R.J.N. Phillips, Phys. Lett. **B335**, 510 (1994).
- [17] F. del Aguila, M.K. Chase and J. Cortes, Nucl. Phys. **B271**, 61 (1986).
- [18] G.C. Branco and L. Lavoura, Nucl. Phys. **B278**, 738 (1986).
- [19] B. Mukhopadhyaya, A. Ray and A. Raychaudhuri, Phys. Lett. **B186**, 147 (1987); **B190**, 93 (1987).
- [20] P. Langacker and D. London, Phys. Rev. **D38**, 886 (1988); P. Langacker, M. Luo and A.K. Mann, Rev. Mod. Phys. **64**, 87 (1992).
- [21] E. Nardi and E. Roulet, Phys. Lett. **B248**, 139 (1990); E. Nardi, E. Roulet and D. Tommasini, Nucl. Phys. **B286**, 239 (1992), Phys. Rev. **D46**, 3040 (1992), Phys. Lett. **B344**, 225 (1995).
- [22] Y. Nir and D. Silverman, Phys. Rev. **D42**, 1477 (1990); D. Silverman, *ibid* **D45**, 1800 (1992); Y. Nir, Phys. Lett. **B327**, 85 (1994).
- [23] L. Bento and G.C. Branco, Phys. Lett. **B245**, 599 (1990); L. Bento, G.C. Branco and P.A. Parada, Phys. Lett. **B267**, 95 (1991).
- [24] G.C. Branco et al., Phys. Rev. **D48**, 1167 (1993), Phys. Lett. **B306**, 398 (1993); G. Bhattacharya, G.C. Branco and D. Choudbury, *ibid* **B336**, 487 (1994), erratum **B340**, 266 (1994).
- [25] W.-S. Choong and D. Silverman, Phys. Rev. **D49**, 2322 (1994).
- [26] G.C. Branco, P.A. Parada and M.N. Rebelo, Vienna preprint UWThPh-1994-51 (January 1995).
- [27] E. Nardi and E. Roulet, Phys. Lett. **B245**, 105 (1990).
- [28] F.J. Gilman, K. Kleinknecht and B. Renk, in *Review of Particle Properties*, Phys. Rev. **D50**, 1315 (1994).

- [29] CDF collaboration: F. Abe et al, Phys. Rev. Lett. **73**, 225 (1994), Phys. Rev. **D50**, 2966 (1994) and FERMILAB-PUB-94/411-E.
- [30] D0 collaboration: S. Abachi et al, Phys. Rev. Lett. **72**, 2138 (1994), FERMILAB-Pub-94/354-E.
- [31] The LEP collaborations ALEPH, DELPHI, L3, OPAL and The LEP Electroweak Working Group, report to Glasgow Conference, July 1994, CERN/PPE/94-187
- [32] OPAL collaboration: M.Z. Akrawy et al, Phys. Lett. **B236**, 364 (1990).
- [33] CDF collaboration: F. Abe et al, Phys. Rev. **D45**, 3921 (1992).
- [34] see e.g. J. Ellis, G.-L. Fogli and E. Lisi, Phys. Lett. **B333**, 118 (1994); J. Erler and P. Langacker, UPR-0632T.
- [35] V. Barger, E. Mirkes, R.J.N. Phillips and T. Stelzer, Phys. Lett. **B338**, 336 (1994).
- [36] M. Gluck, R.M. Godbole and E. Reya, Z. Phys. **C38**, 441 (1988); U. Baur and J.J. van der Bij, Nucl. Phys. **B304**, 451 (1988).
- [37] Particle Data Group, Phys. Rev. **D50**, 1173 (1994).
- [38] S. Narison, CERN-TH.7405/94.
- [39] V. Barger and R.J.N. Phillips, "Collider Physics", Addison-Wesley, New York, 1987.
- [40] K.S. Babu, X.-G. He, X.-Q. Li and S. Pakvasa, Phys. Lett. **B205**, 540 (1988).
- [41] S. Pakvasa, University of Hawaii preprint UH-511-797-94, hep-ph/9408270.
- [42] J.L. Hewett, SLAC preprint SLAC-PUB-6695, hep-ph/9410314.
- [43] A.P. Heinson et al (BNL E791 collaboration), Phys. Rev. **D51**, 985 (1995).
- [44] Fermilab E653 Collaboration, Phys. Lett. **B345**, 85 (1995).
- [45] L.T. Handoko and T. Morozumi, Hiroshima preprint HUPD-9409.

- [46] A.J. Buras, M. Misiak, M. Münz and S. Pokorski, Nucl. Phys. **B424**, 374 (1994); M. Misiak, Nucl. Phys. **B393**, 23 (1993); K. Adel and Y. P. Yao, Mod. Phys. Lett. **A8**, 1679 (1993); M. Ciuchini, E. Franco, G. Martinelli, L. Reina and L. Silvestrini, Phys. Lett. **B316**, 127 (1993).
- [47] N. Cabibbo and L. Maiani, Phys. Lett. **B79**, 109 (1978); M. Suzuki, Nucl. Phys. **B145**, 420 (1978); N. Cabibbo, G. Corbò, and L. Maiani, *ibid* **B155**, 93 (1979).
- [48] See e.g. H.-Y. Cheng, et al., Phys. Rev. **D51**, 1199 (1995) and references therein.
- [49] F. del Aguila and M.J. Bowick, Nucl. Phys. **B224**, 107 (1983).
- [50] W.-S. Hou, A. Soni and H. Steger, Phys. Lett. **B192**, 441 (1987).
- [51] A. Ali and D. London, Talk present at the 27<sup>th</sup> International Conference on High Energy Physics (ICHEP), Glasgow, July, 1994.
- [52] A. Buras, Nucl. Phys. **B347**, 491 (1990).
- [53] L.E. Ibáñez and J. Mas, Nucl. Phys. **B286**, 107 (1987).
- [54] F. del Aguila, G.D. Coughlan, M. Quiros, Nucl. Phys. **B307**, 633 (1988).
- [55] R. Hempfling, Max Planck Institute preprint MPI-PhT/95-9, hep-ph 9502201.
- [56] E. Ma, University of California preprint UCRHEP-T-138, hep-ph 9411408.
- [57] B. C. Allanach and S. F. King, Phys. Lett. **B328**, 360 (1994).
- [58] M. Drees, Nucl. Phys. **B298**, 333 (1988).
- [59] R. Barbieri and G.F. Giudice, Phys. Lett. **B309**, 86 (1993).

TABLES

TABLE I. FCNC effects of singlet quarks

|                          | $Q_x = -\frac{1}{3}$ | $Q_x = \frac{2}{3}$ |
|--------------------------|----------------------|---------------------|
| $K^0-\bar{K}_0$ osc.     | Z-exchange           | box                 |
| $D^0-\bar{D}^0$ osc.     | box                  | Z-exchange          |
| $B_d^0-\bar{B}_d^0$ osc. | Z-exchange           | box                 |
| $B_s^0-\bar{B}_s^0$ osc. | Z-exchange           | box                 |

TABLE II. Quantum numbers of rank 5  $E_6$  models

|  | <b>10</b>     |                |         | <b>5*</b>     |                | <b>1</b>       | <b>5*</b>      |               | <b>5</b>      |                | <b>1</b>       |
|--|---------------|----------------|---------|---------------|----------------|----------------|----------------|---------------|---------------|----------------|----------------|
| Model  | $Q_L$         | $u_L^c$        | $e_L^c$ | $d_L^c$       | $L$            | $\nu_L^c$      | $H$            | $x_d^c$       | $\bar{H}$     | $x_d$          | N              |
| $Y \left( \times \sqrt{\frac{3}{5}} \right)$     | $\frac{1}{6}$ | $-\frac{2}{3}$ | 1       | $\frac{1}{3}$ | $-\frac{1}{2}$ | 0              | $-\frac{1}{2}$ | $\frac{1}{3}$ | $\frac{1}{2}$ | $-\frac{1}{3}$ | 0              |
| $Y' \left( \times \sqrt{\frac{1}{40}} \right)$   | -1            | -1             | -1      | -2            | -2             | 0              | 3              | 3             | 2             | 2              | -5             |
| $Y'' \left( \times \sqrt{\frac{1}{40}} \right)$  | -1            | -1             | -1      | 3             | 3              | -5             | -2             | -2            | 2             | 2              | 0              |
| $Y''' \left( \times \sqrt{\frac{1}{15}} \right)$ | -1            | -1             | -1      | $\frac{1}{2}$ | $\frac{1}{2}$  | $-\frac{5}{2}$ | $\frac{1}{2}$  | $\frac{1}{2}$ | 2             | 2              | $-\frac{5}{2}$ |

## FIGURES

FIG. 1. Unitarity of the  $3 \times 3$  CKM matrix implies triangle relations like the one shown. In  $4 \times 4$  mixing cases the triangle relations become quadrangle relations.

FIG. 2. The  $Z \rightarrow \bar{x}x$  contribution to the total  $Z$  decay width  $\Gamma_Z$  is shown versus  $m_x$  for  $Q_x = -\frac{1}{3}$  and  $\frac{2}{3}$ .

FIG. 3. Singlet quark mixing can give meson-antimeson oscillations via induced FCNC tree diagrams (a) and via box diagrams (b), illustrated here for the  $B_d^0 - \bar{B}_d^0$  case.

FIG. 4. Effects of a  $Q = \frac{2}{3}$  singlet quark on  $b \rightarrow s\gamma$  decay. The branching fraction normalized to the SM value is shown versus the singlet quark mass. The curves are labelled by the values of  $|\hat{V}_{xs}^* \hat{V}_{xb}|$ ; we assume that  $\hat{V}_{xs}^* \hat{V}_{xb}$  and  $\hat{V}_{ts}^* \hat{V}_{tb}$  have the same phase within an overall  $\pm$  sign, shown on the label.

FIG. 5. The CP asymmetry  $\text{Im} \lambda(B_d \rightarrow \psi K_S)$  in the presence of down-type singlet quarks. The band indicates the present uncertainty in the SM prediction. For some values of  $\delta_d$  and  $\theta_{bd}$  (defined by Eq. (83)) there are no solutions as the unitarity quadrangle cannot be made to close.

FIG. 6. The CP asymmetry  $\text{Im} \lambda(B_d \rightarrow \pi^+ \pi^-)$  in the presence of down-type singlet quarks. The entire range is allowed in the SM. The parameters  $\delta_d$  and  $\theta_{bd}$  are defined by Eq. (83).

FIG. 7. One-loop gauge coupling evolution, adding either one  $d$ -type singlet ( $n_{x_d} = 1$ ) or one  $u$ -type singlet ( $n_{x_u} = 1$ ) to the MSSM. The singlets leave the  $SU(2)_L$  gauge coupling unaffected at one-loop, but alter the evolution of the other gauge couplings and destroy unification.

FIG. 8. One-loop and two-loop gauge coupling evolution with the addition of different numbers of light **10** multiplets of  $SO(10)$  to the MSSM. Successful gauge coupling unification is preserved with the addition of one or two **10**-plets, but is threatened by two-loop effects when three light **10**-plets are added to the MSSM.



FIG. 9. Two-loop gauge coupling evolution where the electroweak scale matter consists of three light  $\mathbf{27}$ 's. Gauge coupling unification is unsuccessful without the presence of a light pair of Higgs doublets from a split representation. The result for the case including a pair of light Higgs doublets is shown in Fig. (8).

FIG. 10. The evolution of the top quark Yukawa coupling in the presence of three light  $\mathbf{10}$  multiplets of  $SO(10)$  added to the MSSM. The top quark Yukawa coupling reaches its infrared fixed point for a large range of initial (GUT) values,  $\lambda_{tG}$ . The curves show  $\lambda_{tG}$  between 0.2 and 4 in increments of 0.2.

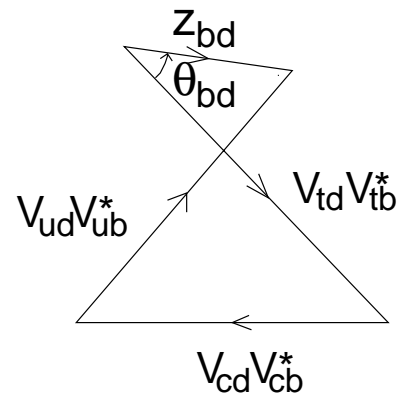
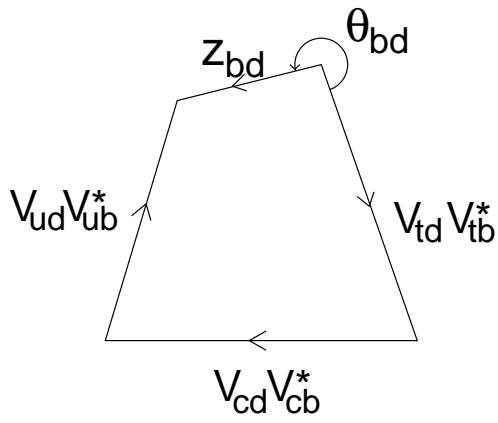
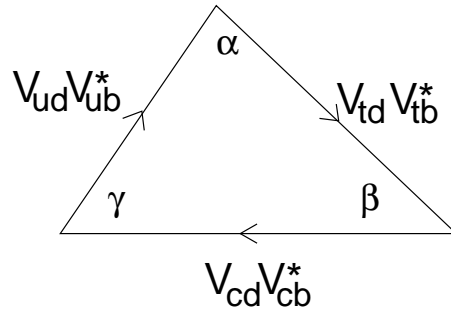


Figure 1

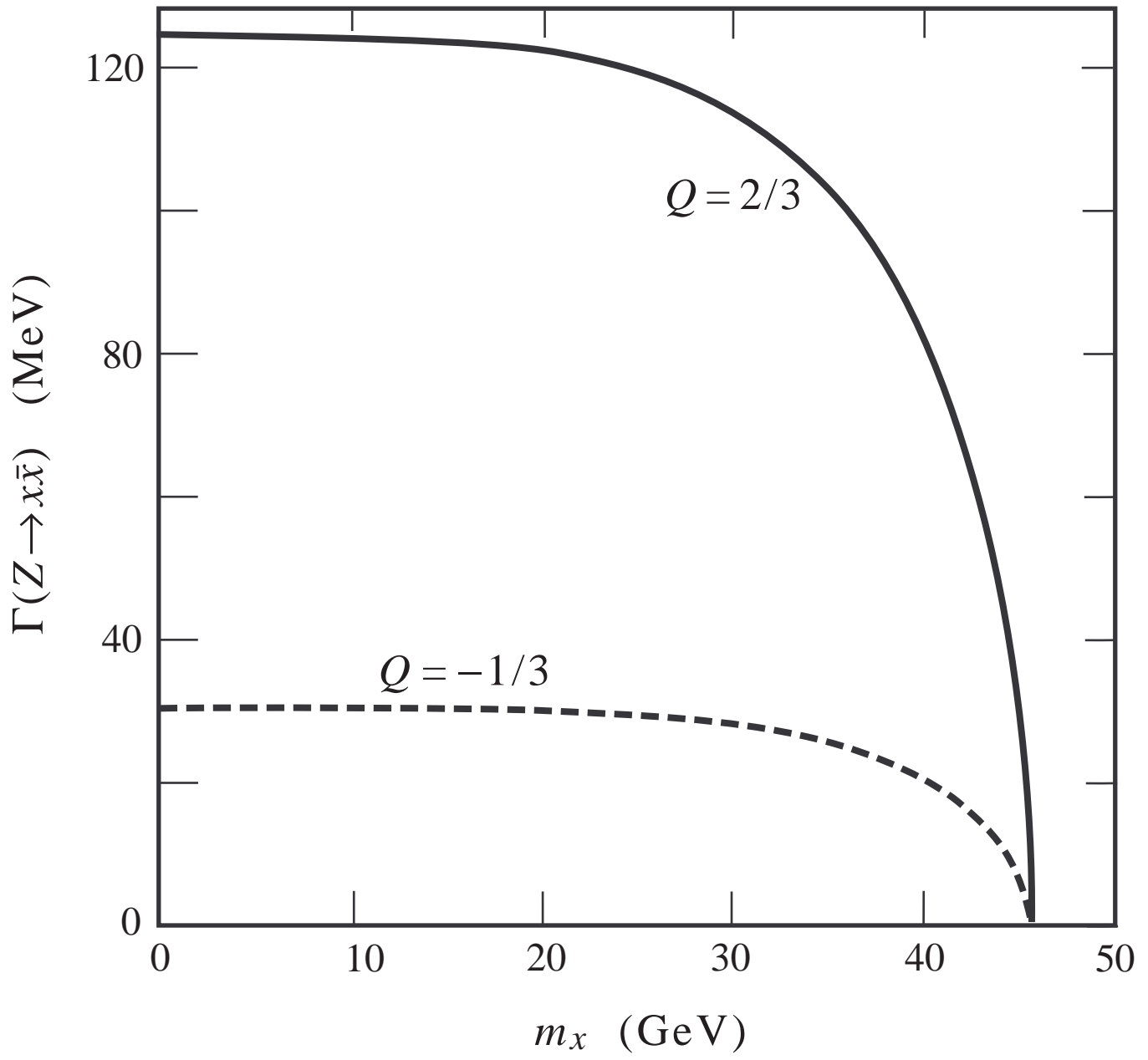
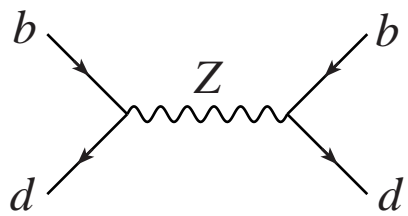
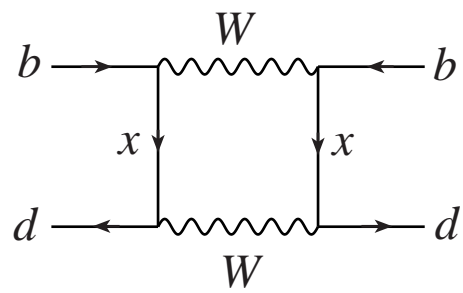


Figure 2



(a)



(b)

Figure 3

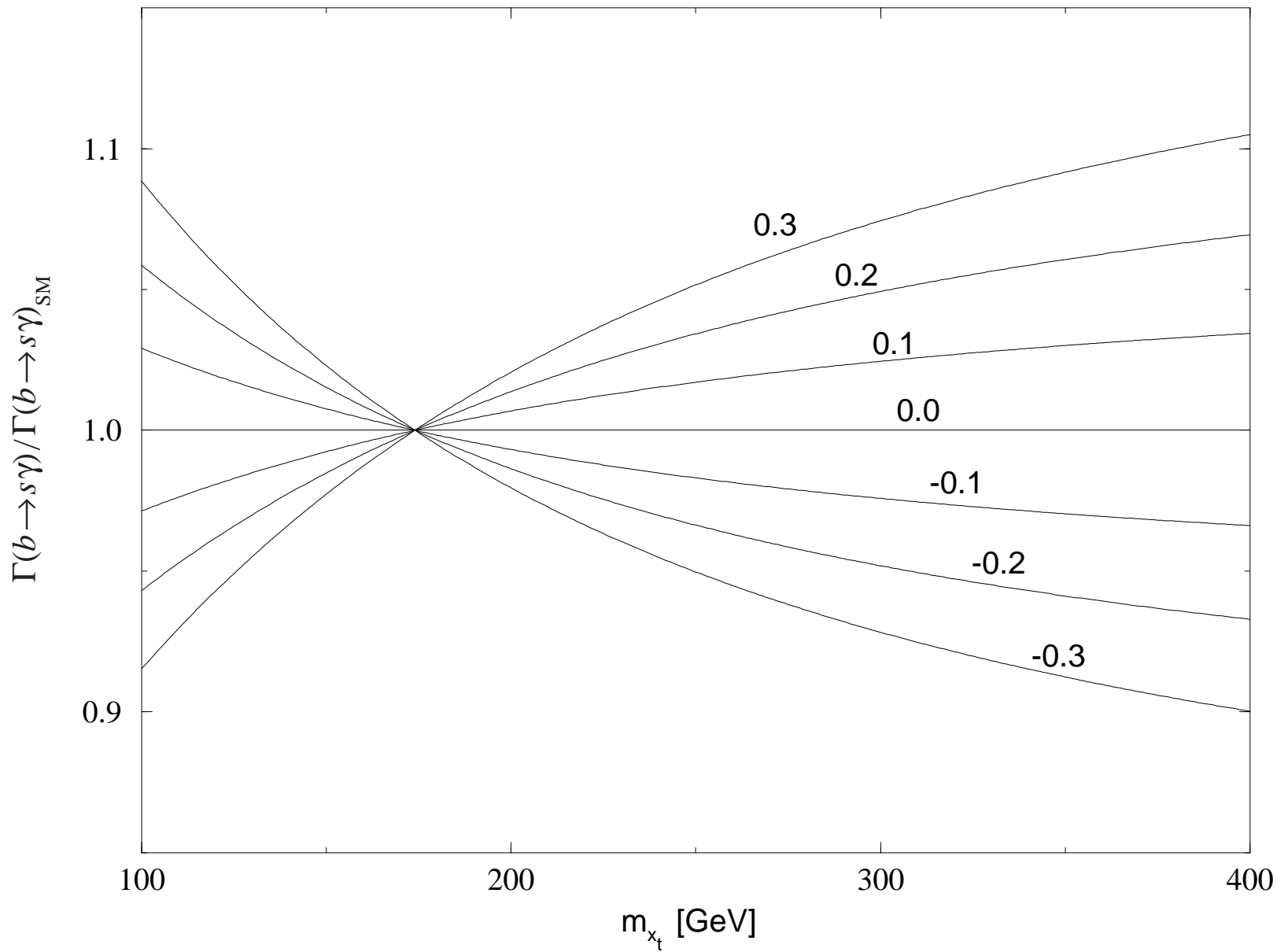


Figure 4

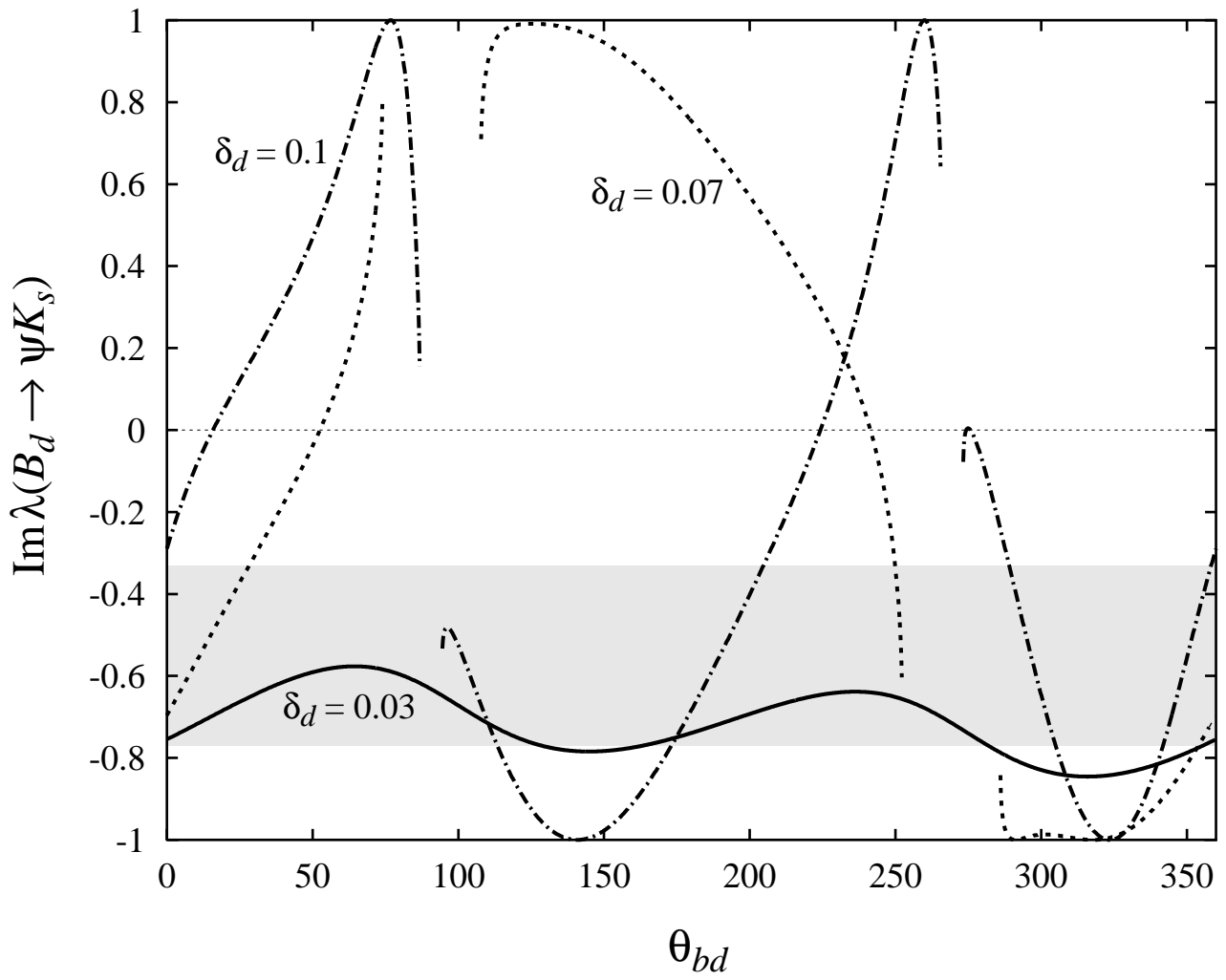


Figure 5

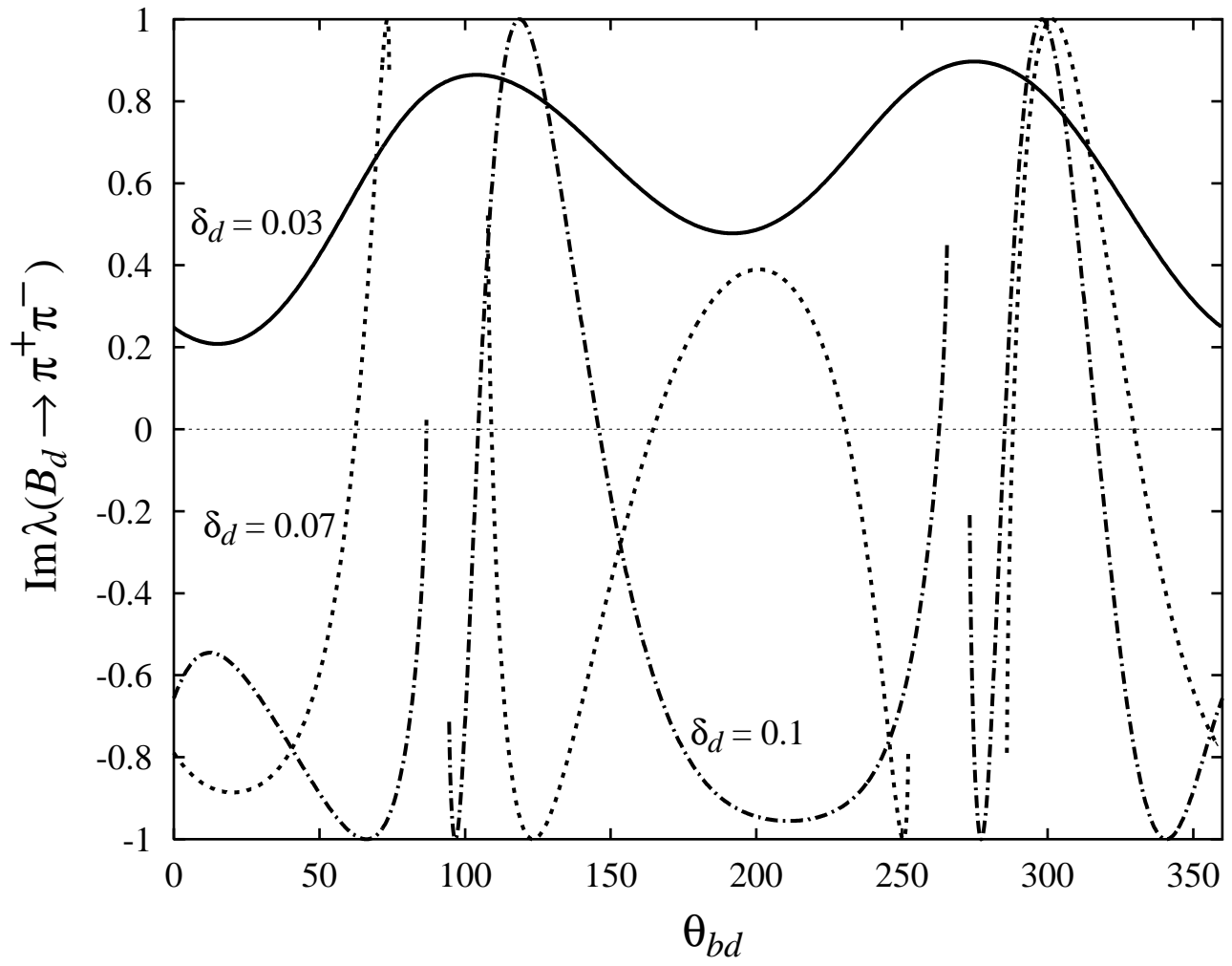


Figure 6

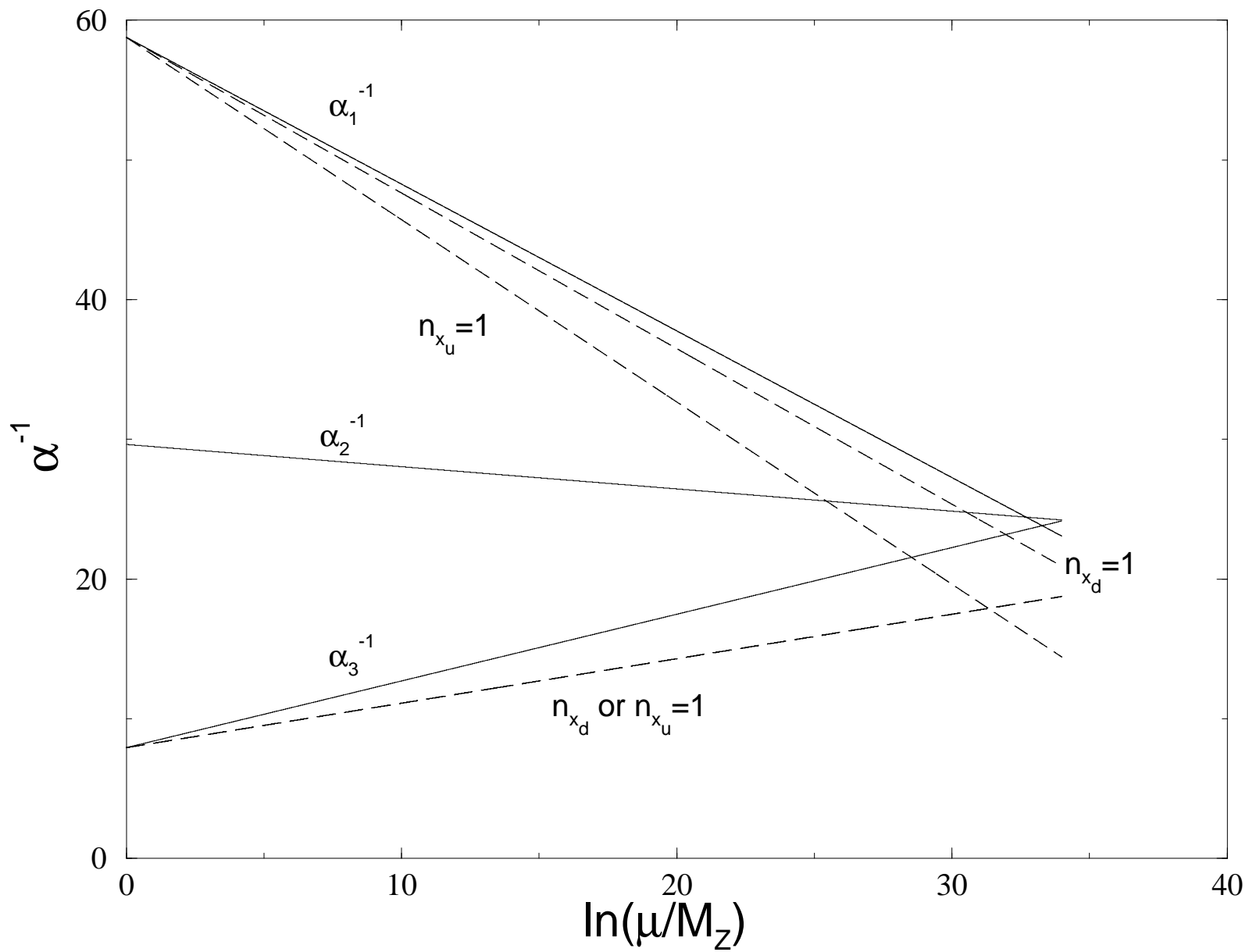


Figure 7



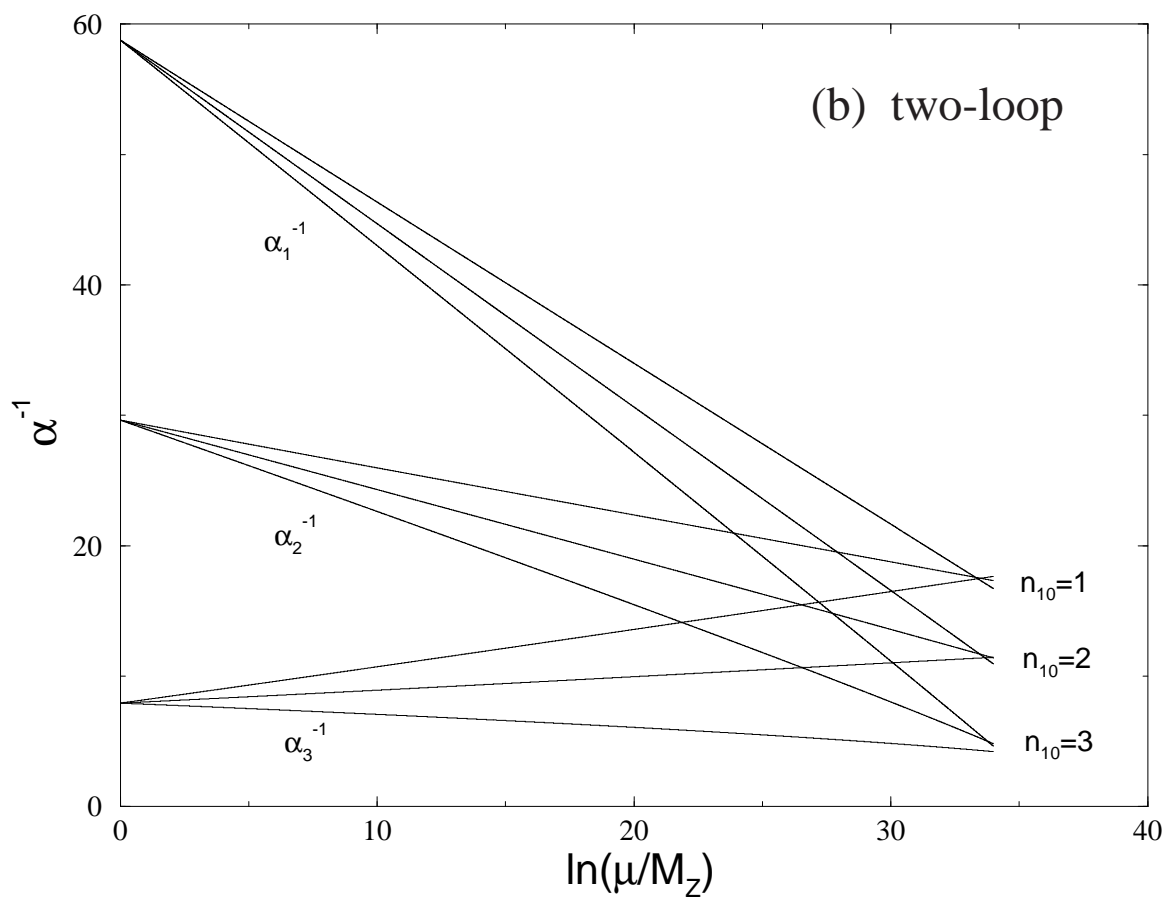
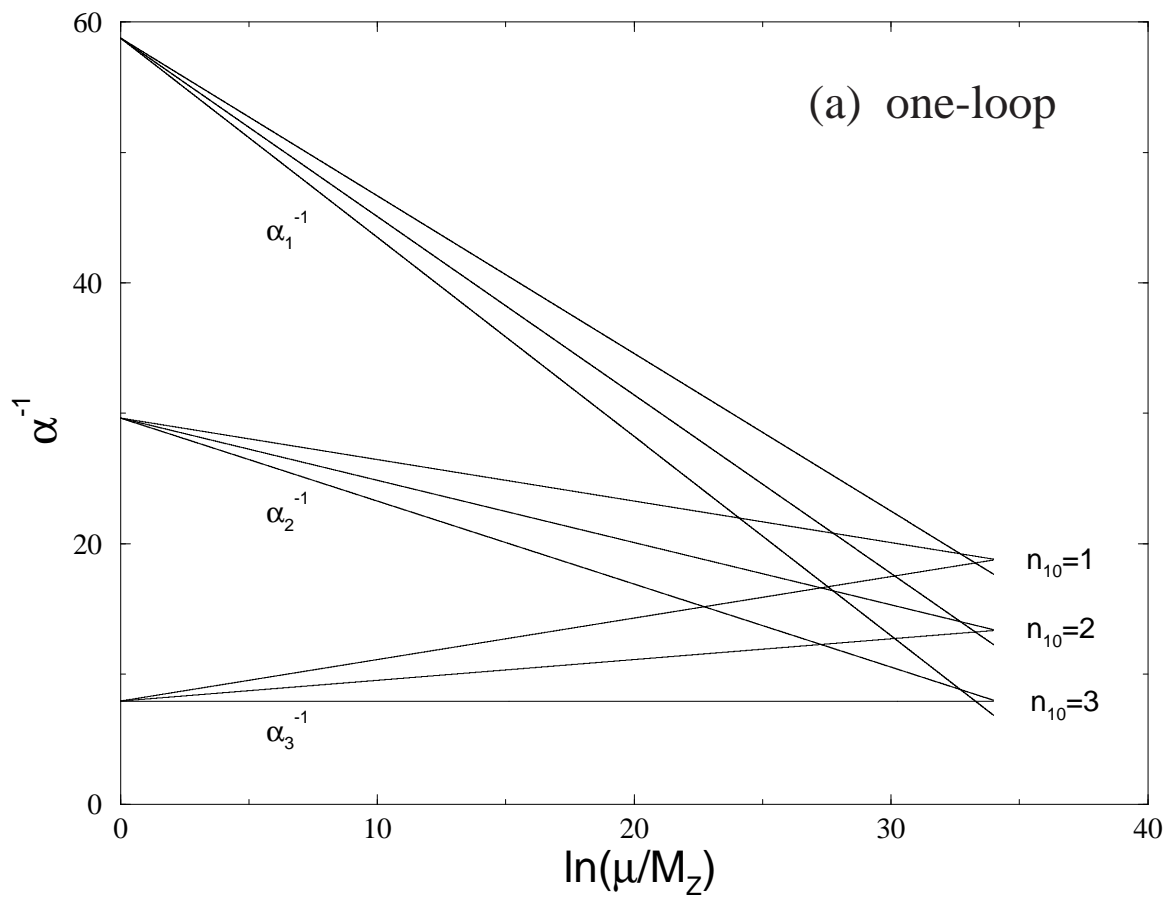


Figure 8

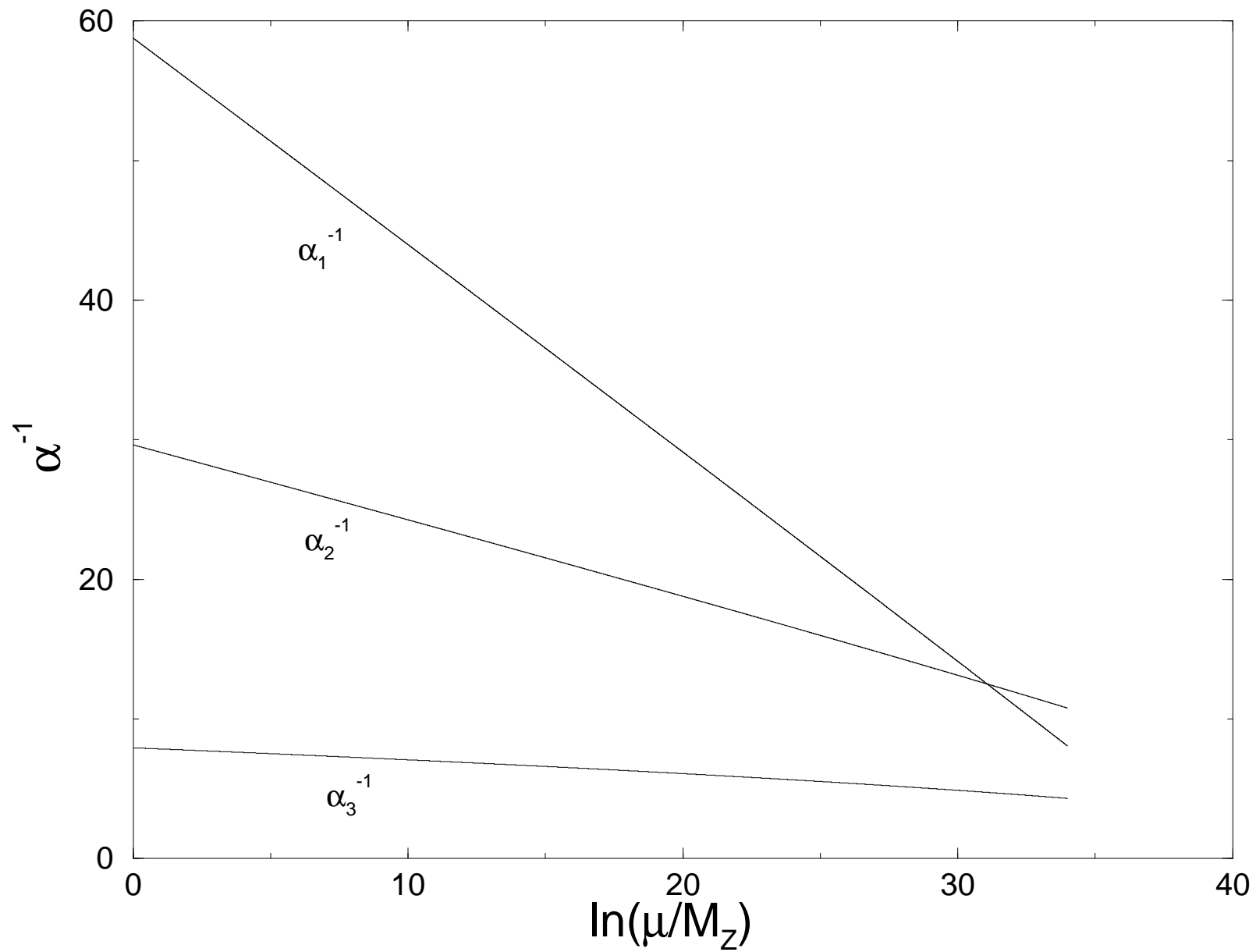


Figure 9

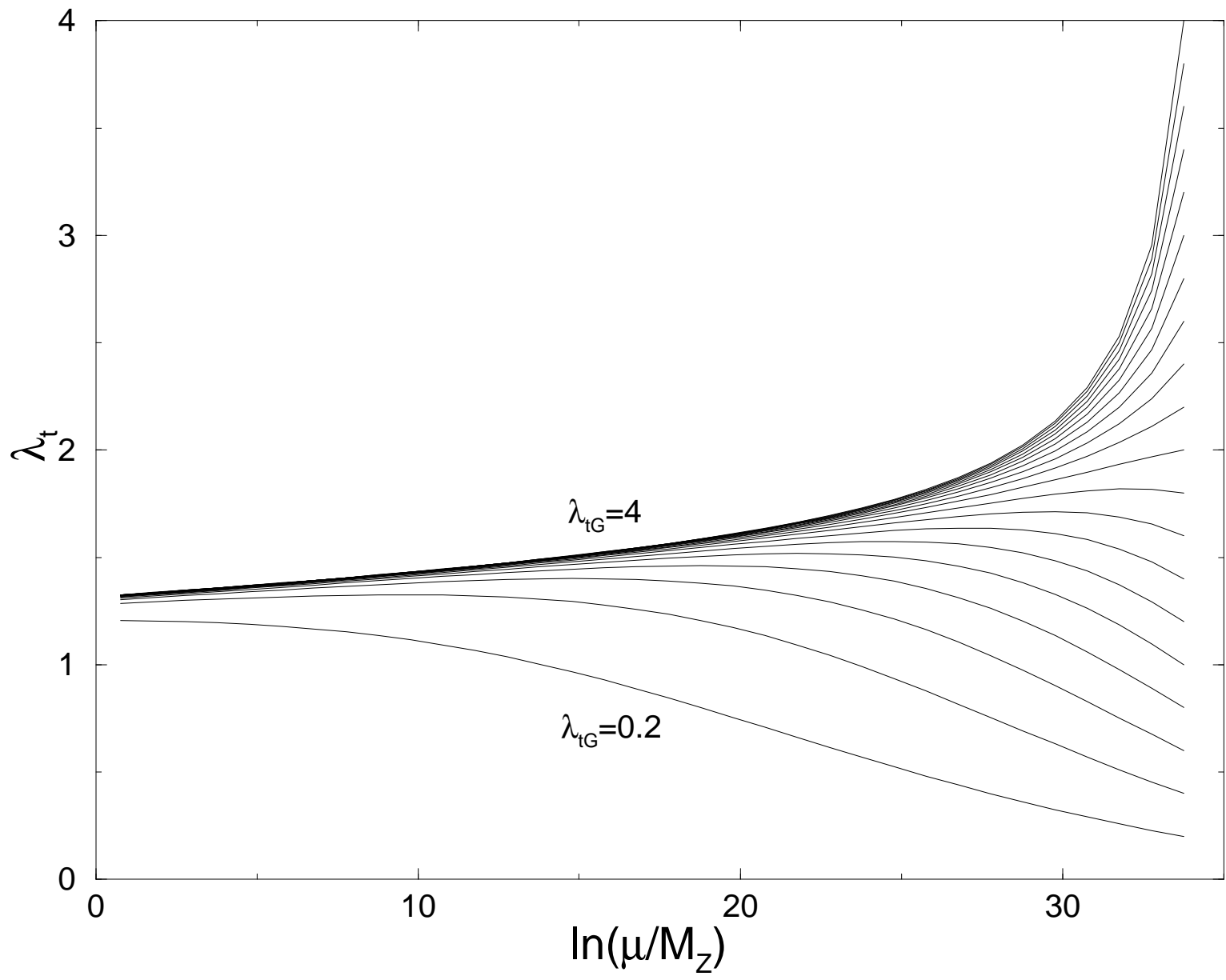


Figure 10